A DISPATCH OPTIMIZATION MODEL FOR HYBRID RENEWABLE AND BATTERY SYSTEMS INCORPORATING A BATTERY DEGRADATION MODEL

by

Sahana Upadhya

A thesis submitted in partial fulfillment of
the requirements for the degree of

Master of Science

(Mechanical Engineering)

at the

UNIVERSITY OF WISCONSIN–MADISON

2021

Date of final oral examination: August 12, 2021

The thesis is approved by the following members of the Defense Committee:
Michael J. Wagner, Assistant Professor, Mechanical Engineering
Gregory F. Nellis, Professor, Mechanical Engineering
Sage L. Kokjohn, Associate Professor, Mechanical Engineering

Approved:

Michael J. Wagner, Assistant Professor of Mechanical Engineering

Dedicated to my family.

ACKNOWLEDGMENTS

My heartfelt thanks to my advisor, Dr. Mike Wagner for patiently hand-holding me throughout this study. Without his able guidance, it would have been impossible to complete this dissertation in a meaningful manner. I would also like to sincerely thank Dr. Greg Nellis, Director, Solar Energy Lab for giving me an opportunity to undertake this research study. And to my family...for always being there!

CONTENTS

LIST OF TABLES

LIST OF FIGURES

DISCARD THIS PAGE

NOMENCLATURE

Term	Definition
DOD	Depth of discharge
EOL	End of life
MILP	Mixed-integer-linear program
PV	Photovoltaic
SOC	State of charge

A DISPATCH OPTIMIZATION MODEL FOR HYBRID RENEWABLE AND BATTERY SYSTEMS INCORPORATING A BATTERY DEGRADATION MODEL

Sahana Upadhya, Master of Science
Department of Mechanical Engineering
University of Wisconsin-Madison, 2021

Assistant Professor Michael J. Wagner, Advisor

The aim of this thesis is to develop a dispatch optimization model for hybrid renewable systems with battery energy storage, maximizing the profits obtained from the dispatch of energy from the system while also considering the degradation of the battery and ensuring its cost-effective usage. An increase in the production of renewable energy has established a need to integrate this technology with battery storage to prevent wastage of energy produced and further increase power dispatch through grid planning. Therefore, research efforts are being channeled into developing a dispatch optimization model for hybrid systems. An important component present in many renewable hybrid systems is a battery for the storage of excess energy to be used when desired. Lithium batteries are commonly used due to their high energy density, but are expensive, and therefore prolonging the life of these batteries through efficient usage is highly beneficial to improve the overall profitability of such models. This establishes a necessity to develop a dispatch model that accounts for battery degradation and ensures the most effective use of the battery.

The degradation of the battery can be understood through two approaches; the theoretical method, exploring the internal structure of the battery (such as the solid electrolyte interphase) and the empirical method, associated with the operational parameters and variables of the battery (such as the state of charge). In addition to this, there is cyclic aging and calendar aging which causes battery degradation. There is still a certain level of ambiguity when it comes to the exact characterization of the aging of the battery and most results are extrapolated from experimental

data, as in the current work. It is also difficult to incorporate all the parameters and variables involved with battery aging in an optimization model as this increases the computational complexity.

A number of dispatch models with battery degradation models have been developed, but many of them use heuristic methods to characterize battery usage. This sacrifices the accuracy with regards to the cost effective use of the battery since the relation between battery parameters and variables that determine the life of the battery, are not included in the optimization model. The dispatch optimization models that do incorporate battery lifetime optimization in the model do so using energy throughput rather than by calculating battery degradation for each cycle of use of the battery. Therefore, in this work, a dispatch optimization model for hybrid renewable systems is developed that incorporates battery degradation with the goal of maximizing profits while also factoring in the cost of eventually replacing the battery based on its use. Battery degradation is characterized by developing an optimization model that explicitly accounts for cyclic aging. Certain key parameters and variables have been chosen based on literature to define the degradation of the battery. The state of charge, depth of discharge and number of cycles of charge and discharge of the battery have been identified as important factors deciding the degradation of the battery, and the capacity fade of the battery is calculated on a per-cycle basis.

The optimization model is developed using Pyomo version 5.6.9 and solved using Gurobi version 9.1.0. In this model, a photovoltaic system is considered. The data for the power generated by the photovoltaic system is obtained from System Advisor Model (SAM)'s PVWatts – Residential Model. The photovoltaic system is connected to the grid and to a battery. Energy generated by the photovoltaic system can be sent to the grid, up to the grid limit, and/or sent to the battery. The battery can then dispatch energy to the grid (ensuring net energy sent to the grid is below the grid limit). The objective of the model is to maximize profits, which are determined by multiplying the power sent to the grid by the cost of electricity (i.e., the price at which electricity is sold to the grid). In addition to revenue, the objective function includes a battery degradation cost that is calculated based on the

cost of eventually replacing the battery, thereby encouraging cost-effective battery usage.

When calculating degradation of the battery due to cyclic aging, a method is needed to count these cycles. The "rainflow algorithm" is commonly used to count and categorize irregular cycles based on desired parameters and variables. This method is compared to a conventional cycle counting method to establish its necessity. The two cycle counting methods predict a difference of 0.044% in battery degradation for a time period of one year. Since this value is negligible, the conventional cycle counting method can be used in the optimization model, thereby avoiding the computational difficulties accompanying the rainflow algorithm.

The efficacy of the model is tested by comparing it with a similar dispatch model without battery lifetime optimization. One year of data is fed into both models, and two primary outcomes are determined: (i) the final battery capacity due to degradation, and (ii) the cumulative objective function which consists of the revenues from power sales minus the costs due to battery degradation and replacement at EOL. The results show that the battery lifetime optimization model extends the battery life significantly. If the degradation trends seen in one year repeat in the following years, the battery without the degradation model would reached EOL in 6 years while the battery with the degradation model would reached EOL in 27 years. In addition to this, the dispatch model with battery lifetime optimization results in a final objective function that is 34.17% higher than the model without battery lifetime optimization, in one year. This demonstrates that batteries play a crucial role in the cost of the system and the model with battery lifetime optimization results in much higher profits when the cost of replacing the battery is considered.

A sensitivity study is carried out to examine the impact of (i) the grid limit of the system, (ii) the cost of the battery, and (iii) the initial battery capacity on the final battery degradation percent and objective function. These studies provide a better understanding of how these parameters effect the model. It is seen that a lower battery cost results in a higher objective function value, as well as a higher extent of battery degradation. A higher grid limit results in an increased objective

function and degradation of the battery. When varying the initial battery capacities, a lower initial capacity gives an improved final objective and increased battery degradation. We observe that in many cases, there is a positive correlation between increased objective and battery degradation. This is due to the fact that increased battery use results in increased energy dispatch, and therefore greater profits, leading to a greater objective function. However, extensive use of the battery also leads to greater degradation. Finally, day-ahead scheduling using a 36 hour horizon produces better results in most cases than a 24 hour horizon, although the difference is not significantly large. We hypothesize that this could be because of the repetitive nature of the power produced by the photovoltaic system day to day, although further tests using longer horizons must be conducted to better understand the viability of day-ahead scheduling.

In conclusion, the advantages of battery lifetime optimization are evident in this work. The use of such battery lifetime optimization models allow for both improved accuracy when factoring in replacement costs and greater net revenue obtained by hybrid systems. The drastic increase in battery life further emphasizes the effectiveness of this modeling approach.

1 INTRODUCTION

As world wealth has been increasing since the industrial revolution (late 19th century), energy consumption has been increasing in an equally exponential manner. A majority of this energy has been obtained from fossil fuels and this has many detrimental implications on the world and the population. Fossil fuels release emissions that cause global warming and are unhealthy when inhaled by any living being. In addition to this, fossil fuels are non-renewable energy sources that are rapidly depleting due to extremely high usage. However, with increased penetration of renewable energy in industry, the global increase in fossil fueled energy consumption will not be as steep, although population and wealth will continue to increase. By 2050, it is predicted that the global increase in energy usage would plateau (Sharma et al., 2019). This suggests a decoupling of the rates of economic growth (steadily increasing) and energy demand growth (ascending but at a slower rate).

Renewable energy is proving to be more economical in many countries as renewable sources are largely available on a local basis while fossil fuels must be imported in many cases. Petroleum based imports accounted for close to 100 billion dollars in USA in 2020 to 2021 (U.S. Census Bureau, Imports of Petroleum, 2021). In addition to this, it is predicted that doubling the share of renewable energy in 2030 would increase the global GDP by about 1.3 trillion dollars (Ferroukhi et al., 2016). This will occur due to increased employment, reduced human-induced environmental calamities, overall better welfare and an improved balance of payments in international trade (Ferroukhi et al., 2016). The average solar photovoltaic (PV)

plant has twice the number of jobs per unit generation when compared to a coal generation plant (Ferroukhi et al., 2016). As of 2019, fossil fuels accounted for 84 percent of energy consumption worldwide, but as the world energy consumption increases on a yearly basis, renewable energy contributes largely to the percentage increase (41 percent in 2019) (bp Statistical Review of World Energy, 2021). These statistics clearly emphasize the importance of renewables for the world health and economic development.

The amount of energy produced by renewable power production systems is dependent on the source of the renewable energy; for example, solar energy on the sun and wind energy on the wind. These sources, being natural occurrences, cannot be controlled and result in the variable nature of renewable energy. The variability in energy produced by renewable systems can be reduced with the use of energy storage systems such as batteries. Battery technology is developing rapidly, with increased interest in lithium-ion battery technology due to its high energy density. However, attempts are being made to increase the life of batteries, which is dependent on operating decisions, such as number of charge and discharge cycles and state of charge (SOC). Therefore, by manipulating these decision, the battery can be used efficiently and the lifetime of the battery can be extended. In this work, we attempt to use the battery in a more effective manner to extend the lifetime.

The steady increase in the use of renewable energy has led to a change in the electricity demand to be met by grid operators. This change is variable and is dependent on the energy produced by the renewables. The variability in renewable energy production has led to the manifestation of the so-called “duck curve”

(Denholm et al., 2015, 2008). The duck curve is a graph representing the electric power demand of specific markets. Initially, when the use of renewable energy was almost negligible, the curve (Figure 1.1) shows lower energy demand during the night, which gradually increases as the day progresses (as seen in year 2012). As the use of renewable energy has increased, a mid-day dip in the net energy demand on the grid has appeared due to high solar energy production, which leaves dispatchable electricity production plants with a challenge. Grid operators are increasingly forced to curtail solar power production during mid-day, since conventional plants (for example, those run by fossil fuels) cannot always be rapidly stopped and started to accommodate the excess solar energy produced. This, in turn, has led to the wastage of solar energy and emphasizes the need to integrate variable renewables on the grid system planning and operation in order to maximize the use of renewable power generation.

One path for accommodating variable renewables is the adoption of hybrid systems comprised of a renewable generator such as wind or PV alongside a battery storage system, and such systems are now of increasing interest commercially. The development and integration of such systems in the dispatch of power produced to the grid allows grid operators to more efficiently plan the dispatch of energy, thereby reducing the wastage of energy due to overproduction. In addition to this, there has been a growing interest in developing stand-alone hybrid systems for power production in remote areas that may or may not be connected to the utility grid. Such systems tackle the irregularities in power supply and allow an increased use of renewables for power production (Lasseter, 2007). The integration of two or

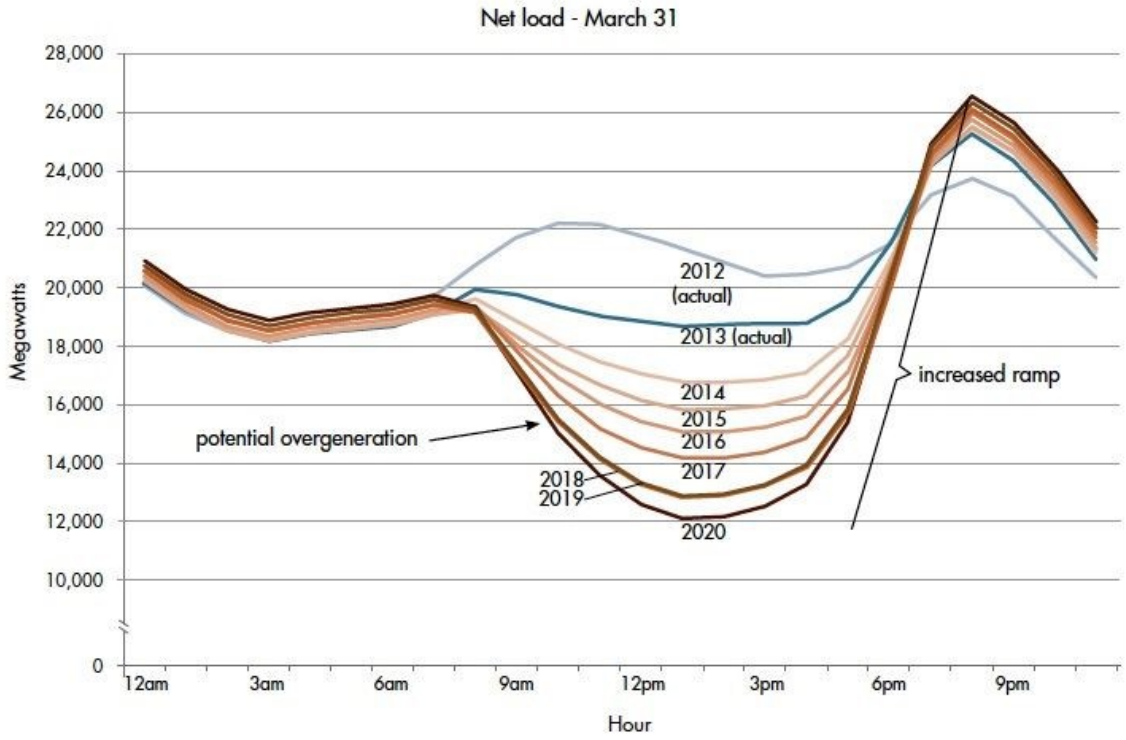

Figure 1.1: DUCK CURVE SHOWING ELECTRIC POWER DEMAND FROM YEARS 2012 TO 2020 (Denholm et al., 2015)

more power systems is complex, and without efficient utilization, the investment into such a system may not be rational (Fathima and Palanisamy, 2015). Therefore optimization models must be developed to ensure the most cost effective dispatch of energy from hybrid systems. In addition to this, lithium-ion batteries, which are the common battery of choice in hybrid systems, are expensive. The incorporation of battery degradation models in a dispatch optimization model for hybrid systems, can further improve the cost efficiency of the hybrid systems and increase net revenue. However, the development of battery degradation models is challenging as degradation is a function of decisions being made in the model, which includes

the charge and discharge of the battery. This results in a non-linear relationship which can be challenging to make linear and solve. The process also involves counting of cycles which requires analyzing a horizon of time steps which, in turn, increases the computational time of the model. This work attempts to overcome these challenges. In light of this, we have developed an optimization model for PV-plus-battery hybrid systems that also accounts for degradation of the battery and optimizes its use thereby extending its life. This is accomplished by developing a mixed-integer-nonlinear program that has been linearized and implemented with a rolling time horizon to reduce computational time. An equation characterizing capacity degradation of the battery with respect to certain key variables is developed. Finally, the model maximizes profit from electricity sales while also ensuring the most cost-effective usage of the battery.

System description

The system considered in this model can be seen in Figure 1.2 and consists of a PV system connected to the grid through an inverter and to a battery. The battery is connected to the grid through an inverter. The model considers the energy generated by the PV system and choose to send this energy to the grid or to the battery for storage. The model can choose to dispatch energy from the battery to the grid, while ensuring the net energy sent to the grid is below the grid limit.

The model in this work is only concerned with the power flow into the inverter and does not extend beyond that boundary. Therefore, we do not consider the internal working of the inverter, such as inverter losses or behavior. The system

considered in this model can be seen in Figure 1.2 within the dashed lines. The model limits the total power being sent to the inverter, and the power sent to the inverter is then sent to the grid. Therefore, in this model, the "grid limit" is synonymous with the "inverter limit."

The degradation of the battery capacity is calculated for every charge and discharge action as a function of the starting and ending SOC for each charge or discharge cycle and the number of charge or discharge cycles that have occurred. These variables have been chosen based on literature associated with battery lifetime and degradation. The loss associated with the degradation of the battery capacity is considered by multiplying the fractional degradation with the cost of replacing the battery. The model's profit is calculated by multiplying the energy sent to the grid to the cost of electricity and to a revenue multiplier that differs every hour. The objective is to maximize the net profit obtained. Therefore, the model considers all the working variables (via a set of constraints), calculates the battery degradation and the cost associated with this degradation, subtracts this cost from the profit made through energy dispatch, and maximizes the net profit. In doing so, it weighs the benefits of using the battery against the drawbacks of degrading the battery.

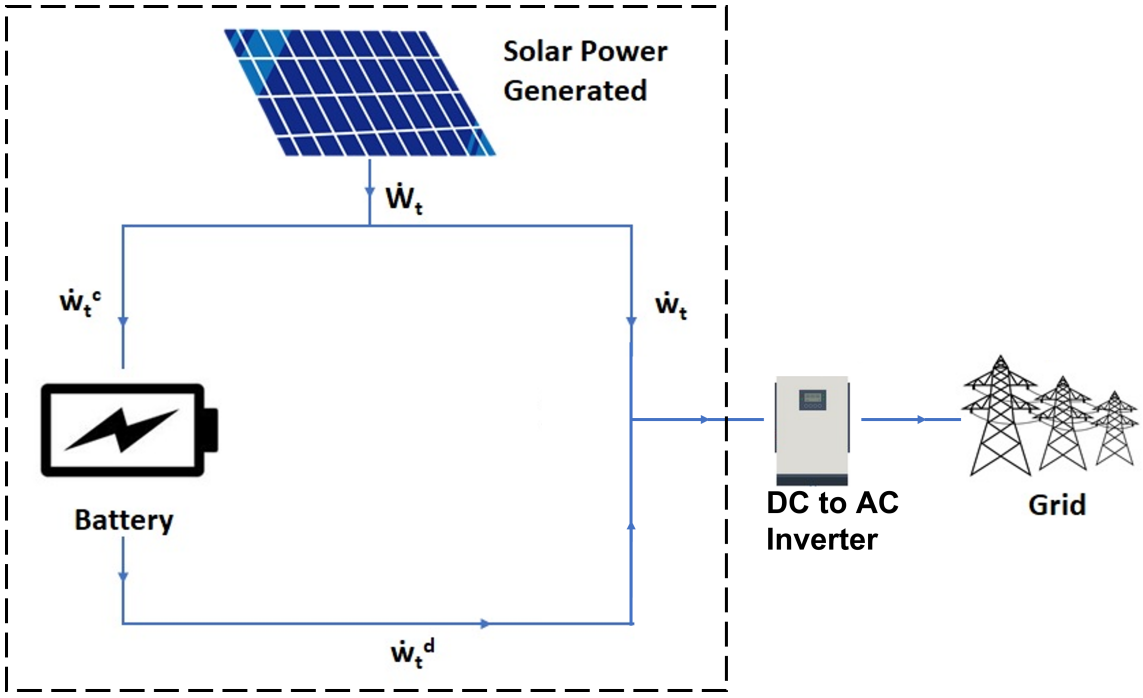

Figure 1.2: WORKING MODEL OF THE POWER GENERATING SYSTEM BEING CONSIDERED IN THIS THESIS. POWER GENERATED BY THE SOLAR PANEL IS SENT TO THE GRID THROUGH THE INVERTER OR TO THE BATTERY FOR STORAGE. THE MODEL CAN DIPATCH POWER FROM THE BATTERY TO THE GRID THROUGH THE INVERTER AS LONG AS IT DOES NOT CROSS THE GRID LIMIT.

2 LITERATURE REVIEW

The work done in this thesis can broadly be divided into two areas of study: an optimization model for the dispatch of power for the entire system and a degradation model to quantify the capacity fade of the battery. Both the models are combined into a single dispatch optimization model that accounts for battery degradation. In the literature review, the first part focuses on previous work of optimization models incorporating battery degradation and how the model in this thesis differs from past work. The second part dwells on research into battery degradation and how various internal and external factors effect the degradation in the battery capacity.

Extensive research efforts are being channeled into developing optimization models integrating renewable energy into the grid system. Some of these models consider battery storage but set a maximum and minimum limit on the battery SOC (Ghorbanzadeh et al., 2019; Zhao et al., 2013). Therefore, the battery is used as desired, up to a designated value, and then stops. This is a heuristic method of optimization, and such methods are governed by pre-determined rules that do not guarantee solution optimality. SAM employs a heuristic approach to battery lifetime optimization in its dispatch model as well (DiOrio et al., 2018). It sets a maximum and minimum SOC, current and power for the charge and discharge of the battery respectively. In this method, the battery degradation is not being characterized in the optimization problem and therefore the optimum trade-off between profits made from battery discharge and the cost of replacing the battery at the end of life (EOL) is not established.Therefore, such models sacrifices optimality and accuracy for speed.

In the work of Maheshwari et al. (2020), degradation is calculated taking into consideration the rate at which current is charged or discharged from the battery and the SOC of the battery. The degradation of the battery due to current rate is determined by comparing it to degradation (d_t^{1C}) that will be caused in the battery for the same change of state at 1C current rate (obtained from experimental data). Therefore, the term d_t^{1C} accounts for variations in degradation due to different SOC as it assumes a different value for different SOC. The actual current rate is determined at every time interval and is translated into a scaling factor that assumes the value 1 at 1C rate and 0 at no load condition (0C). The degradation of the battery at each time step is determined as the product of the scaling factor and d_t^{1C}. This work uses a multi-objective model. The model calculates the revenue obtained from dispatch of power and the degradation of the battery (as explained above). The revenue and the degradation are scaled to be in the same order of magnitude. Both the terms are multiplied by a weighting factor that varies from 0 to 1, wherein one term is multiplied by the complement of the other. Therefore, the revenue obtained by the model and the degradation of the battery establish an inverse weighting in the objective function. The weighting factor carries out a parametric sweep to generate Pareto-optimal scheduling strategies. A number of different weighting factors are tested to calculate the profit obtained versus the degradation of the battery. In this method, the degradation of the battery is not added to the financial calculations and therefore the tradeoff between the cost associated with battery degradation and the profit from the storage of power is not being analyzed at every time step. Rather, a weighting factor decides the priority of the two values

(revenue and degradation) in the objective function for the entire horizon and various weighting functions are calculated and compared to choose an optimum weighting factor.

Merei et al. (2013) models an off-grid hybrid PV–Wind–Diesel system with three different battery types: lead-acid, lithium-ion, and vanadium redox-flow. The lithium-ion battery model computes the voltage of one cell using the SOC, current rate and the temperature of the battery, based on the work of Buller et al. (2003). This model considers the effect of ageing of the battery. The battery capacity and cell resistance is updated and an ageing factor is calculated to determine when to replace the battery. The parameters and variables used in the work of Merei et al. (2013), to determine the aging of the battery are different from those used in this work. The present work considers battery aging based on a per cycle basis, whereas the work of Merei et al. (2013) uses current rate to determine the aging. In addition to this, temperature is not considered as a factor in this work, since the present work focuses on cyclic aging and not calendar aging. Finally, their work employs a genetic algorithm using Matlab and Simulink rather than an MILP optimization model.

Goodall et al. (2019) developed a model to optimize the design and dispatch of a microgrid consisting of batteries, PV and diesel generators. The model meets the power demand on the system while also incorporating the effect of temperature and battery capacity fade. It was found that at higher temperatures, battery resistance is lower. This improves the efficiency but also increases the capacity fade, thereby increasing overall operating costs. It was also noted that higher capacity fade

corresponds to an increase in objective function, while low values of capacity fade show negligible increase in objective function. While this model optimizes the use of the battery, it uses operational variables that differ from the work in this thesis to do so. The model does not optimize on a per-cycle usage but by using energy throughput. This is also the case in the work of Goebel et al. (2016).

Goebel et al. (2016) implements a highly detailed battery degradation model, characterizing both cyclic and calendar aging. The equations used in their paper are derived from accelerated lifetime tests of the battery available elsewhere in literature. Calendar aging is derived as a function of the duration in months, the storage temperature and the resting SOC of the battery. This relation was derived from the work of Swierczynski et al. (2015). The capacity fade of the battery due to cyclic aging is calculated based on an expression introduced by Wang et al. (2011). This equation relates the battery capacity fade to the battery capacity throughput, the surface temperature and the C-rate of the battery. The work of Goebel et al. (2016) differs from the work in this thesis, once again, in the fact that it does not optimize the model on a per-cycle basis. The degradation is characterized using different battery operational variables. In addition to this, Goebel et al. (2016) characterizes calendar aging and although this makes the model more detailed and accurate, it is computationally complex, hindering its use in long-term planning studies.

Different battery parameters and variables affect the degradation of the battery in different ways in battery lifetime optimization. For example, when considering charge throughput in a battery degradation model, depth of discharge (DOD)

has a negligible effect on degradation (Wang et al., 2011). This is not true when considering charge and discharge cycles, and DOD plays a significant role in the model discussed in this work.

Therefore our work attempts to design a power dispatch model that maximizes profits while optimizing the battery usage by incorporating the degradation relations in the constraints and objective function. The degradation of the battery is calculated based on variables identified in existing literature as being crucial in determining the life of the battery.

When designing any power system with storage for an application, one of the areas of high investment cost is batteries (Schoenung, 2011). Lithium-ion batteries are emerging as a commonly used grid-scale storage technology because of favorable characteristics such as high energy density, extended cycle life and their capability of operating over a large temperature range (Goodenough and Kim, 2010). However, with extended usage, the batteries undergo a reduction in capacity and increase in internal resistance (Ouyang et al., 2016; Barré et al., 2013; Palacín and de Guibert, 2016; Lu et al., 2013). A large amount of effort is being devoted to developing techniques to understand and reduce the degradation of batteries, thereby extending their lifetime.

There are fundamentally two approaches for understanding the degradation of batteries: the theoretical method and the empirical method. The theoretical method explores the internal structure of the battery. Herein, aging of the battery is associated with side reactions occurring between the electrolyte and the electrodes (Kassem et al., 2012; Belt et al., 2011; Ploehn et al., 2004). Cycling-induced

degradation is correlated to the fatigue of the solid electrolyte interphase layer due to the intercalation and de-intercalation of lithium in the graphite active material (Laresgoiti et al., 2015). Empirical methods, on the other hand, correlate operational characteristics such as the DOD and SOC to degradation (Xu et al., 2016; Millner, 2010; Ghorbanzadeh et al., 2019; Fortenbacher et al., 2014). However, there is an insufficient amount of information to link operation-level observations to the molecular-level degradation of lithium-ion batteries (Smith et al., 2014; Laresgoiti et al., 2015). Due to this lack of translatability between the two concepts, the empirical method is often used when designing optimization models for power systems. For the purpose of this thesis, as well, the empirical model is adopted.

There are two types of battery degradation: calendar aging and cyclic aging. Calendar aging is the permenant loss of battery capacity over time due to all processes that lead to degradation independent of charge or discharge of the battery. Calendar aging is predominantly due to the chemical degradation of the battery induced at higher ambient temperatures and the SOC level at which the battery is allowed to rest at for a period of time (Xu et al., 2016). Cyclic aging is the degradation of the battery with every cycle of charging and discharging. Cyclic aging is affected by the DOD, SOC at the starting and ending of a charge cycle as well as the number of cycles completed by the battery. Ecker et al. (2014), shows that cyclic aging affects the capacity and resistance of a battery more drastically than calendar aging (Ecker et al., 2014) and is therefore further discussed below.

One of the factors that influences cyclic aging is DOD. Lower DOD increases the life of the battery (Wikner and Thiringer, 2018) and reduces the capacity fade.

For example, when going from 100% DOD to 50% DOD, a four-fold improvement of cycle life is observed due to decreased capacity fade. Cycle life of a battery is the number of cycles (charge and discharge together being considered a single cycle) a battery can complete before it reaches EOL. In order to establish a more comparable term for varying DOD, EOL is also evaluated using equivalent full cycles which is the cumulative capacity discharge divided by the battery rated capacity. The reduced DOD also shows a three-fold improvement in expected number of equivalent full cycles (Guena and Leblanc, 2006). In addition, lower or higher SOC's are seen to accelerate degeneration and reduce the life of batteries (Ecker et al., 2014; Wikner and Thiringer, 2018; Zheng et al., 2015). Finally, it has been found that minimizing the number of cycles of charge-discharge also reduces the amount of degradation of the battery (Bordin et al., 2017).

Therefore, this work develops an optimization model, formulated as a MILP, incorporating battery cyclic aging on a per-cycle basis. The battery degradation model in this study penalizes high and low SOC and number of cycles of charge and discharge to correctly characterize the battery degradation. By incorporating this battery degradation model in the dispatch model, the objective function (the total profit) calculated factors in the eventual cost of replacing the battery based on the degradation and the EOL of the battery. This is, therefore, a more accurate portrayal of the net profit.

3 MODEL METHODOLOGY

In this thesis, we develop a rolling-time-horizon mixed-integer-linear optimization model for a hybrid system, with the objective of maximizing profits and minimizing the degradation of the battery and the cost associated with eventually replacing it. The model maximizes energy dispatched to the grid while not exceeding the grid interconnection limit. The system being considered for optimization consists of a solar PV system and an electrochemical battery. The entire system is connected to the grid for dispatch, but does not allow electricity purchase from the grid. The schematic of the system is shown in Figure 1.2 (on page 7). The optimization model is developed using Pyomo version 5.6.9 and solved using Gurobi version 9.1.0. The objective of the linear program is to maximize profits obtained from the dispatch of power. The data for the power generated by the PV system is obtained from System Advisor Model (SAM)'s PVWatts – Residential Model (Freeman et al., 2018). SAM is a software tool developed by the National Renewable Energy Lab (NREL) for predicting the productivity of integrated power plants over the course of a year using weather data from the National Solar Resource Database (Sengupta et al., 2018). It is a performance and financial model used to estimate the cost of energy and facilitates the decision-making process by making performance predictions in renewable power generating systems. The power generated at each hour by the PV system as modeled by SAM is shown in Figure 3.1, and this is used as an input in the hybrid optimization model being developed in this thesis.

The objective is to develop a model that decides the dispatch of the energy gener-

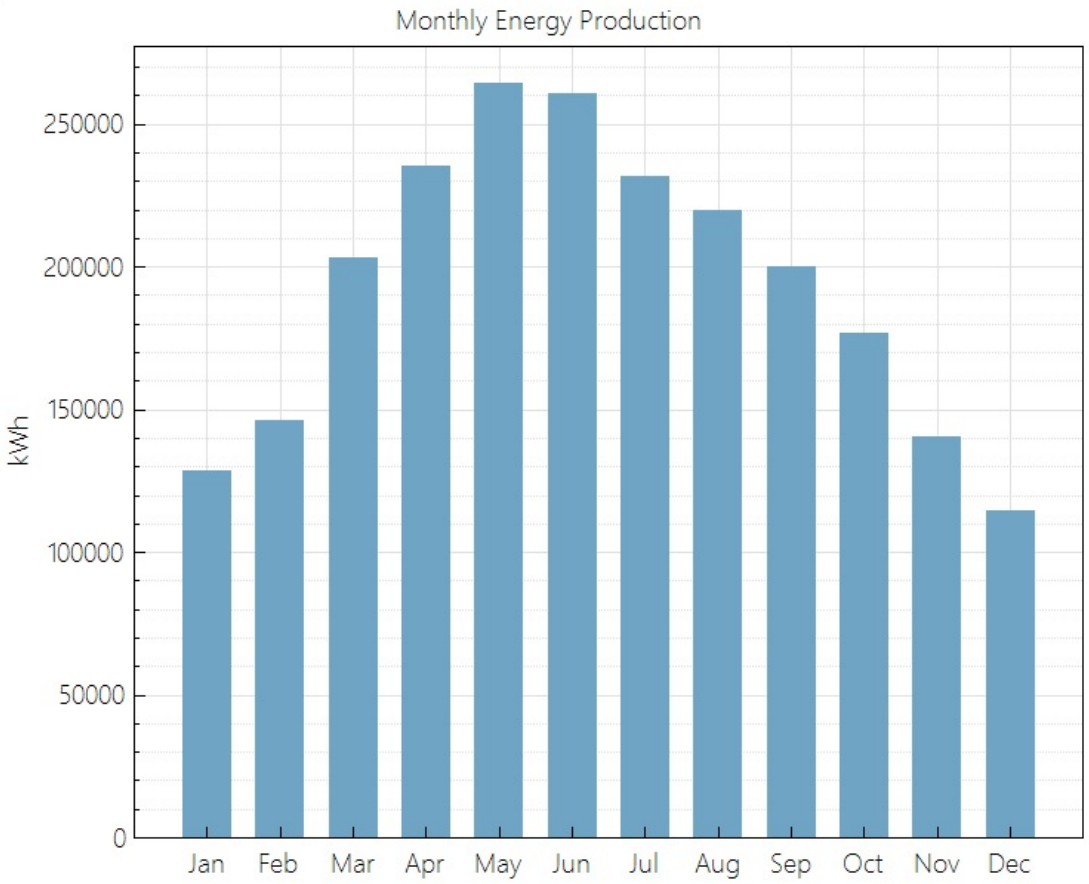

Figure 3.1: PV WATTS MONTHLY ENERGY PRODUCTION DATA PRODUCED BY SAM. THE POWER IN KWH FOR EACH MONTH OF THE YEAR IS TABULATED.

ated by the system, maximizing the profitability, while considering the degradation of the battery due to cyclic aging.

The challenge in characterizing battery degradation exists in relating the operational variables to those associated with the aging of the battery. To accomplish this, we study experimental data from literature linking the prominent factors in use of a battery such as SOC, DOD and cycles completed, to the capacity of the battery. This

data is used to develop constraints relating the capacity of the battery to the starting and ending SOC of the battery and the number of cycles of charge and discharge. Each cycle of charge and discharge is evaluated, and the peaks and troughs of the graph are recorded using binary variables whose state corresponds to the SOC of the battery. This is collated to a single binary variable whose state reflects the start and end of a half-cycles, which is further used to calculate the loss in capacity of the battery. This loss is then incorporated in the objective function using a cost function. A rolling optimization approach is used with a time horizon of 36 hours and an update period of 24 hours. Larger horizons pose an increased computation time. Therefore, a 36 hour horizon was chosen to capture the next-day effects without an exorbitant computational time. Decisions are made within the problem horizon, but only 24 hours of decisions are registered in order to avoid "end effects." The horizon then rolls forward by another 24 hours, and the optimization problem is again solved. This method is commonly used for day-ahead market scheduling.

Mathematical model

Table 3.1: SETS

Symb.	Description
T	Set of all time steps in the optimization window $\{1 \ldots N_T\}$
$\hat{T}$	Two-dimensional set of all time steps in the optimization window $\{t, t \ldots N_T\}$

Sets: A set is the solution space of the problem and signifies all the possible points in the optimization window that satisfy the constraints in the problem. It is the

initial set of possible solutions which is further narrowed down by the model. Two sets have been established in this problem. The set T is the set of time steps that run from 0 to N_T , wherein N_T is equal to the time horizon used in the model. This set is applied to all the one-dimensional variables. Further, a second set $\hat{T}$ is defined relative to the first set (T). This set is used to represent two-dimensional variables that are defined by a combination of two time steps. The set $\hat{T}$ is defined as all the combinations of the time step t and t to N_T, as shown in Eq. 3.1.

$$\hat{T} = (t, \hat{t}) \; \forall \hat{t} \in \{t \dots N_T\}, \; \forall t \in T \tag{3.1}$$

Therefore, through this set, a single variable can relate two time steps. This has been established to be able to capture the time step for the start and end of a half-cycle in a single two-dimensional variable.

Parameters: Parameters are pre-defined inputs fed in the model. They are used to characterize the physical aspects of the system such as the cost of electricity (K) or the power produced by the PV system $(\dot{W}_t)$. These values are fixed in the optimization window. The big M is a a number chosen to be larger than the greatest value that can be assumed by the variables associated with it in the constraint (Eq. (3.16)), that is, in this case, the battery degradation. The value of big M depends on the greatest obtainable battery degradation (Eq.'s (3.14a-3.15b). Therefore, the big M value is determined as follows:

Table 3.2: PARAMETERS

Symb.	Units	Description
Δ	-	(Fractional hours) time step duration
η	-	Charge or discharge efficiency
γ	-	Constant used in symmetry breaking
ϵ	-	Binary variable weighting constant
A_i	-	Battery degradation constraint (Eq. 3.14a-3.15b) regression constant $i \in \{0 \dots 2\}$
K	\$/kW-hr	Baseline revenue for electricity sold
L	-	Allowable battery degradation before required replacement at EOL (fractional)
M		Big M
N_T	hrs	Magnitude of Set T
P	\$	Cost of the battery
S^N	kW-hr	Initial battery capacity before any degradation
S	kW-hr	Battery capacity at the beginning of an optimization time horizon (updated over time)
$S0$	kW-hr	Energy in battery storage at the initial optimization time horizon time step
U_1	kW	Unit multiplier
$\dot{W}_t$	kW	Power production from the PV system at time t
$\dot{W}^g$	kW	Maximum power that the grid can accept
Z_t	-	Revenue multiplier for electricity sold at time t

$$M = -A_1 \cdot 100 \cdot 0.5 - \frac{A_2 \cdot 0.5}{100} \tag{3.2}$$

Variables: A number of continuous and binary variables have been introduced to appropriately model the physical constraints on the system and the degradation of the battery based on literature. The variables, their symbols, and their units are summarized in Table 3.3.

Table 3.3: VARIABLES

Symb.	Units	Description
Continuous variables		
$\kappa_{t,\hat{t}}$	-	Degradation of the battery capacity value at every time step (fractional)
κ_t^f	-	Capacity of the battery at each time step t (fractional)
s_t	kW-hr	Energy stored in battery at time t
$y_{t,\hat{t}}$	-	Degradation of the battery capacity due to charge or discharge cycles (fractional)
$\dot{w}_t$	kW	Power from PV sent to the grid at time t
$\dot{w}_t^c$	kW	Power sent to charge battery at time t
$\dot{w}_t^d$	kW	Power from battery discharge at time t
Binary variables		
β_t		1 if battery is discharging in time t, 0 otherwise
θ_t		1 if battery is charging in time t, 0 otherwise
f_t		1 if battery is neither charging nor discharging in time t, 0 otherwise
$G_{t,\hat{t}}$		1 if t, $\hat{t}$ is the starting and ending point of a charge or discharge cycle respectively, 0 otherwise

$\dot{w}_t$ signifies the amount of power generated by the PV system that is sent to the grid. The model is also given the flexibility to send the power produced by the PV system to the battery and this is represented by $\dot{w}_t^c$. On the contrary, when the power produced by the PV system is below the grid limit, the power stored in the battery may be discharged and is represented by $\dot{w}_t^d$. The discharge of power to the grid from the battery also depends on the revenue multiplier parameter (Z_t). The model attempts to discharge the battery in the time steps with a higher revenue multiplier so as to maximize profits. s_t is the amount of energy stored in the battery at time t and is calculated based on the amount of power entering the battery ($\dot{w}_t^c$) and leaving the battery ($\dot{w}_t^d$).

To incorporate the battery degradation model, a number of binary variables have been defined. These, too, eventually affect the charge and discharge of the battery. θ_t assumes the value of 1 for every time step in which battery charging is occurring and 0 otherwise. β_t assumes the value of 1 for every time step in which battery discharging is occurring and 0 otherwise. f_t assumes the value of 1 when neither charging nor discharging is occurring and 0 otherwise. It is essential to describe the action (charging, discharging, or steady) of the battery at every time step through these binary variables to facilitate tracking the time step in which charging or discharging begins and ends. These binaries (θ_t, β_t and f_t) are used to identify battery cycles by constraining the values of a two-dimensional binary variable $G_{t,\hat{t}}$. $G_{t,\hat{t}}$ uses the other binary variables to assume the value 1 when t represents the start of charge or discharge cycle and $\hat{t}$ represents the end of the corresponding charge or discharge cycle, respectively. $G_{t,\hat{t}}$ takes the value of 0 in cases where a charge or discharge cycle does not start and end at t, $\hat{t}$. In this manner, a single indexed variable establishes the presence of a charge or discharge half-cycle in its entirety. The equation characterizing $G_{t,\hat{t}}$ (Eq.)3.16)) is formulated such that a half-cycle with interspersed steady state periods ($f_{t^\star} = 1,\ t^\star \in \{t \dots \hat{t}\}$), is accounted for as a single half-cycle rather than a number of half-cycles. $G_{t,\hat{t}}$ then allows the identification of the starting and ending SOC of every half-cycle which is subsequently used to calculate the degradation of the battery, represented by the variable $\kappa_{t,\hat{t}}$. The degradation that would be realized is calculated for every $t, \hat{t}$ combination irrespective of whether or not that combination eventually represents a half-cycle, using the SOC at t and $\hat{t}$ as the starting and ending SOC. $\kappa_{t\hat{t}}$ is then used

to constrain the continuous variable $y_{t\hat{t}}$ which is 0 when no half-cycle is taking place and nonzero only when $t, \hat{t}$ represent the starting and ending point of a charging or discharging half-cycle. This is done using the big M (M). The big M (M) is used along with a binary variable (in this case, $G_{t,\hat{t}}$) in Eq. (3.16) to constrain the value of $y_{t,\hat{t}}$ based on whether the binary variable is true (1) or false (0). When $G_{t,\hat{t}}$ assumes the value 1, the big M value is multiplied by 0 allowing the value of $y_{t,\hat{t}}$ to be chosen by the model based in the $\kappa_{t,\hat{t}}$ value. When $G_{t,\hat{t}}$ assumes the value 0, the big M value is multiplied by 1 and being associated with a negative value, forces $y_{t,\hat{t}}$ to 0. This allows $y_{t,\hat{t}}$ to be conditional based on the value of $G_{t,\hat{t}}$. Finally, κ_t^f is used to track the change in capacity of the battery at every time step with respect to the previous time step.

Objective function: In an optimization model, the objective is a function to be maximized or minimized subject to a number of constraints. In the current model, Eq (3.3) is the objective function wherein the goal is to maximize profits and minimize battery replacement costs. The total energy sent to the grid from the battery or directly from the PV array is multiplied by the cost of electricity (K) and a revenue multiplier (Z_t). In addition, the degradation of the battery, $y_{t,\hat{t}}$ is calculated as the fraction of degradation with respect to the updated battery capacity (S) in every update period. This is converted to the fraction of degradation based on the initial battery capacity (S^N). Further, it is divided by the EOL (L) to calculate the fraction of allowable degradation. This is finally associated with a negative value and multiplied by a term representing the cost of replacing the battery (P). Further, the capacity of the battery at every time step, κ_t^f, is added to

maximize this value at every time step, to optimize battery usage. In this manner, κ_t^f, and $y_{t,\hat{t}}$ favor maximizing the battery capacity and reducing the degradation of the battery, thereby increasing the lifetime of the battery. The other binary variables are intermediate variables and are added in the objective function to encourage them to act in a meaningful manner. These variables are the binary variables associated with the state of the battery and are θ_t, β_t and f_t.Finally γ and ϵ are symmetry-breaking and weighting constants, respectively: γ is used to favor power generated, being sent to the grid directly rather than power going to the grid through the discharge of the battery; ϵ is used to incentivize the desired state of the binary variables when equivalent solutions are present.

Maximize:

$$\begin{aligned}\sum_{t\in T}\left[\left(\dot{w}_t+\gamma\cdot\dot{w}_t^d\right)\cdot Z_t-\left(\left(f_t+\theta_t+\beta_t\right)\cdot\epsilon-\kappa_t^f\right)\cdot U_1\right]\cdot K\\ -\sum_{t,\hat{t}\in\hat{T}}\left[\frac{y_{t,\hat{t}}\cdot P\cdot S}{L\cdot S^N}+G_{t,\hat{t}}\cdot K\cdot\epsilon\cdot U_1\right]\end{aligned} \tag{3.3}$$

Constraints: Following the objective function, a list of constraints must be defined. These are a number of mathematical conditions or restrictions that must be satisfied to ensure the model is functioning in a logical and realistic manner. They represent various physical limitations in a mathematical form and play a very important role in impacting the decision variables.

Power dispatch constraints:

$$\dot{w}_t + \dot{w}_t^d \leqslant \dot{W}^g \quad \forall\, t \in T \tag{3.4}$$

$$(\dot{w}_t^c \cdot \eta - \frac{\dot{w}_t^d}{\eta}) \cdot \Delta = s_t - s_{(t-1)} \quad \forall\, t \in T : t \geqslant 2 \tag{3.5a}$$

$$(\dot{w}_1^c \cdot \eta - \frac{\dot{w}_1^d}{\eta}) \cdot \Delta = s_1 - S0 \tag{3.5b}$$

$$s_t \leqslant S \quad \forall\, t \in T \tag{3.6}$$

$$\dot{w}_t + \dot{w}_t^c \leqslant \dot{W}_t \quad \forall\, t \in T \tag{3.7}$$

Eq.'s (3.3-3.24) represent the basic optimization model developed. The constraints span from Eq.'s (3.4-3.24). Some of the constraints have been split into parts *a* and *b* to account for the first or last time step wherein certain variables assume the value 0. Eq. (3.4) ensures that the sum of power from the PV system ($\dot{w}_t$) and that from the battery discharge ($\dot{w}_t^d$) is less than the grid limit for all time steps. In Eq. (3.5a), power entering ($\dot{w}_t^c$) and leaving ($\dot{w}_t^d$) the battery translates into the energy stored in the battery (s_t) for every time step greater than 1. The first time step is accounted for by Eq. (3.5b). Eq. (3.6) ensures that the battery SOC(s_t) does not exceed the maximum capacity of the battery (S). The total power is conserved through Eq. (3.7).

Battery cycle constraints:

$$s_t - s_{t-1} \leqslant min(S, \dot{W}_t) \cdot \theta_t \quad \forall\, t \in T : t \geqslant 2 \tag{3.8a}$$

$$s_1 - S0 \leqslant min(S, \dot{W}_1) \cdot \theta_1 \tag{3.8b}$$

$$s_{t-1} - s_t \leqslant min(S, \dot{W}^g) \cdot \beta_t \quad \forall\, t \in T : t \geqslant 2 \tag{3.9a}$$

$$S0 - s_1 \leqslant min(S, \dot{W}^g) \cdot \beta_1 \tag{3.9b}$$

$$\begin{aligned} f_t \cdot S \geqslant\ & 1 + s_t - s_{t-1} - \beta_t \cdot min(S, \dot{W}^g) \\ & - \theta_t \cdot min(S, \dot{W}_t) \quad \forall\, t \in T : t \geqslant 2 \end{aligned} \tag{3.10a}$$

$$\begin{aligned} f_1 \cdot S \geqslant\ & 1 + s_1 - S0 - \beta_1 \cdot min(S, \dot{W}^g) \\ & - \theta_1 \cdot min(S, \dot{W}_1) \end{aligned} \tag{3.10b}$$

$$\theta_t + \beta_t + f_t \leqslant 1 \quad \forall\, t \in T \tag{3.11}$$

$$
\begin{aligned}
G_{t,\hat{t}} \geqslant\ & (\beta_{t-1} - \beta_t) + (\beta_{\hat{t}+1} - \beta_{\hat{t}}) \\
& + \sum_{\bar{t} \in \{t \dots \hat{t}\}} (\theta_{\bar{t}} + f_{\bar{t}}) - (\hat{t} - t) - 2 \\
& \forall\, t, \hat{t} \in \hat{T} : t \geqslant 2,\ \hat{t} \leqslant N_T - 1
\end{aligned} \tag{3.12a}
$$

$$
\begin{aligned}
G_{1,\hat{t}} \geqslant\ & (-\beta_1) + (\beta_{\hat{t}+1} - \beta_{\hat{t}}) \\
& + 1 \cdot \frac{\sum_{t' \in \{1 \dots \hat{t}\}} (\theta_{t'})}{N_T} \\
& + \sum_{\bar{t} \in \{1 \dots \hat{t}\}} (\theta_{\bar{t}} + f_{\bar{t}}) - (\hat{t} - 1) - 2 \\
& \forall\, t, \hat{t} \in \hat{T} : t = 1,
\end{aligned} \tag{3.12b}
$$

$$
\begin{aligned}
G_{t,N_T} \geqslant\ & (\beta_{t-1} - \beta_t) + (-\beta_{N_T}) \\
& + 1 \cdot \frac{\sum_{t' \in \{t \dots N_T\}} (\theta_{t'})}{N_T} \\
& + \sum_{\bar{t} \in \{t \dots N_T\}} (\theta_{\bar{t}} + f_{\bar{t}}) - (N_T - t) - 2 \\
& \forall\, t, \hat{t} \in \hat{T} : \hat{t} = N_T,
\end{aligned} \tag{3.12c}
$$

$$
\begin{aligned}
G_{1,N_T} \geqslant\ & (-\beta_1) + (-\beta_{N_T}) \\
& + 2 \cdot \frac{\sum_{t' \in \{1 \dots N_T\}} (\theta_{t'})}{N_T} \\
& + \sum_{\bar{t} \in \{1 \dots N_T\}} (\theta_{\bar{t}} + f_{\bar{t}}) - (N_T - 1) - 2
\end{aligned} \tag{3.12d}
$$

$$G_{t,\hat{t}} \geqslant (\theta_{t-1} - \theta_t) + (\theta_{\hat{t}+1} - \theta_{\hat{t}}) + \sum_{\bar{t}\in\{t\ldots\hat{t}\}} (\beta_{\bar{t}} + f_{\bar{t}}) - (\hat{t} - t) - 2 \quad \forall\, t, \hat{t} \in \hat{T} : t \geqslant 2,\ \hat{t} \leqslant N_T - 1 \tag{3.13a}$$

$$G_{1,\hat{t}} \geqslant (-\theta_1) + (\theta_{\hat{t}+1} - \theta_{\hat{t}}) + 1 \cdot \frac{\sum_{t'\in\{1\ldots\hat{t}\}}(\beta_{t'})}{N_T} + \sum_{\bar{t}\in\{1\ldots\hat{t}\}} (\beta_{\bar{t}} + f_{\bar{t}}) - (\hat{t} - 1) - 2 \quad \forall\, t, \hat{t} \in \hat{T} : t = 1, \tag{3.13b}$$

$$G_{t,N_T} \geqslant (\theta_{t-1} - \theta_t) + (-\theta_{N_T}) + 1 \cdot \frac{\sum_{t'\in\{t\ldots N_T\}}(\beta_{t'})}{N_T} + \sum_{\bar{t}\in\{t\ldots N_T\}} (\beta_{\bar{t}} + f_{\bar{t}}) - (N_T - t) - 2 \quad \forall\, t, \hat{t} \in \hat{T} : \hat{t} = N_T \tag{3.13c}$$

$$G_{1,N_T} \geqslant (-\theta_1) + (-\theta_{N_T}) + 2 \cdot \frac{\sum_{t'\in\{1\ldots N_T\}}(\beta_{t'})}{N_T} + \sum_{\bar{t}\in\{1\ldots N_T\}} (\beta_{\bar{t}} + f_{\bar{t}}) - (N_T - 1) - 2 \tag{3.13d}$$

Equations (3.8a-3.8b) and Eq.'s (3.9a-3.9b) determine the binary variable value for charge (θ_t) and discharge (β_t) respectively. Eq.'s (3.10a-3.10b) represents the binary variable for steady state (f_t), that is, neither charge nor discharge. This is done by comparing the SOC of the battery (represented by s_t) in the time step t,

with the SOC of the battery in the previous time step. If the SOC is greater in t than in $t-1$ it signifies charging of the battery and θ_t assumes the value 1. If not, θ_t assumes the value 0. The similar occurs for β_t, except a reduce in SOC of the battery results in β_t assuming the value 1. No change in SOC from one time step to the next results in f_t attaining the value of 1. Eq. (3.11) ensures that the charge, discharge and steady state binary variables do not assume the value of 1 in the same time step. Eq.'s (3.12a-3.12d) and (3.13a-3.13d) introduce and evaluate the binary variables $G_{t,\hat{t}}$. Eq. (3.12a) ensures $G_{t,\hat{t}}$ attains the value of 1 for every $t, \hat{t}$ combination in which charging takes place. Similarly, Eq. (3.13a) represents $G_{t,\hat{t}}$ for the discharge half cycles. Eq.'s (3.12b-3.12d) and Eq.'s (3.13b-3.13d) represents $G_{t,\hat{t}}$ at different combination of time step $t = 0$ and $\hat{t} = N_T$. The $G_{t,\hat{t}}$ constraint has been developed such that the end of a charge cycle is considered the beginning of a discharge cycle and the beginning of a charge cycle is the end of discharge. The similar is true for the a charge cycle. Since one half-cycle depends on the half-cycle before and after it, the first and last cycle must be handled differently. To accommodate this, Eq.'s (3.12b-3.12d) and Eq.'s (3.13b-3.13d) have been introduced.

Battery Degradation Constraints:

$$\begin{aligned}\kappa_{t,\hat{t}} \geqslant -(&A_0 \cdot s_{t-1} + A_1 \cdot s_{\hat{t}} \\ &-A_1 \cdot S \cdot (1 - \frac{\sum_{t' \in \{t \dots \hat{t}+1\}} (\theta_{t'} + f_{t'})}{\hat{t} - (t+1)}) \cdot \frac{0.5}{S} \\ &-\frac{A_2 \cdot 0.5 \cdot G_{t,\hat{t}}}{100\%} \quad \forall\, t, \hat{t} \in \hat{T} : t \geqslant 2 \end{aligned} \tag{3.14a}$$

$$\begin{aligned}\kappa_{1,\hat{t}} \geqslant -(&A_1 \cdot s_{\hat{t}} \\ &-A_1 \cdot S \cdot (1 - \frac{\sum_{t' \in \{1 \dots \hat{t}+1\}} (\theta_{t'} + f_{t'})}{\hat{t} - 2}) \cdot \frac{0.5}{S} \\ &-\frac{A_2 \cdot 0.5 \cdot G_{t,\hat{t}}}{100\%} \quad \forall\, t, \hat{t} \in \hat{T} : t = 1 \end{aligned} \tag{3.14b}$$

$$\begin{aligned}\kappa_{t,\hat{t}} \geqslant -(&A_1 \cdot s_{t-1} + A_0 \cdot s_{\hat{t}} \\ &-A_0 \cdot S \cdot (1 - \frac{\sum_{t' \in \{t \dots \hat{t}+1\}} (\beta_{t'} + f_{t'})}{\hat{t} - (t+1)}) \cdot \frac{0.5}{S} \\ &-\frac{A_2 \cdot 0.5 \cdot G_{t,\hat{t}}}{100\%} \quad \forall\, t, \hat{t} \in \hat{T} : t \geqslant 2 \end{aligned} \tag{3.15a}$$

$$\begin{aligned}\kappa_{1,\hat{t}} \geqslant -(&A_0 \cdot s_{\hat{t}} \\ &-A_0 \cdot S \cdot (1 - \frac{\sum_{t' \in \{1 \dots \hat{t}+1\}} (\beta_{t'} + f_{t'})}{\hat{t} - 2}) \cdot \frac{0.5}{S} \\ &-\frac{A_2 \cdot 0.5 \cdot G_{t,\hat{t}}}{100\%} \quad \forall\, t, \hat{t} \in \hat{T} : t = 1 \end{aligned} \tag{3.15b}$$

$$y_{t,\hat{t}} \geqslant \kappa_{t,\hat{t}} - M \cdot (1 - G_{t,\hat{t}}) \;\; \forall\, t, \hat{t} \;\in\; \hat{T} \tag{3.16}$$

$$\kappa_t^f \begin{cases} = 1 & : \; t = 1 \\ \leqslant 1 - \sum_{t' \in \{0 \ldots t\}} (y_{t',t}) & \forall\, t \in T : t \geqslant 2 \end{cases} \tag{3.17}$$

Equations (3.14a-3.15b), have been derived from the data produced in the research studies of Wikner and Thiringer (2018). A graph of the percentage of retention of capacity of the battery versus the number of cycles of the battery for various start and end SOC is used to derive a relation between the variables and the degradation percent of the battery. This relation is expressed in Eq.'s (3.14a -3.15b) and it calculates the fractional capacity degradation of the battery for every $t, \hat{t}$ combination. The equation is divided by 100 to convert it from a degradation percent to fractional degradation. Since this is calculated for each half-cycle (charge or discharge) the number of cycles term is chosen as 0.5 representing one half-cycle. Separate equations are required to evaluate the value of degradation due to charging of the battery and discharging of the battery. Equation (3.14a) represents the degradation due to charging for all values of t greater than 1. Eq. (3.14b) represents the degradation due to charging for t equal to 1. The similar is represented by Eq.'s (3.15a-3.15b) for degradation due to discharge of the battery. $\kappa_{t,\hat{}}$ attains a value of degradation for every $t, \hat{t}$ combination irrespective of whether degradation actually occurs in the particular $t, \hat{t}$ combination or not. Therefore, $\kappa_{t,\hat{t}}$ cannot be used directly in the objective function to account for degradation of the battery. This is made further applicable through Eq. (3.16) wherein $y_{t,\hat{t}}$ assumes a value for capacity degradation for every $t, \hat{t}$ combinations where charge or discharge is

occurring and 0 for every other combination.

Finally, κ_t^f has been established to maintain a comprehensive value of degradation at every time step and is calculated using $y_{t,\hat{t}}$, in Eq. (3.17). This term reflects the battery capacity independently for every time step, with respect to the battery capacity of the previous time step and is not a progressive total capacity.

Cuts:

$$\sum_{t' \in \{0 \ldots t\}} (G_{t',t}) \leqslant O_t + B_t + f_t \quad \forall\, t \in T \tag{3.18}$$

$$\theta_t \leqslant \dot{w}_t^c \quad \forall\, t \in T \tag{3.19}$$

$$\theta_t \cdot \dot{W}_t \geqslant \dot{w}_t^c \quad \forall\, t \in T \tag{3.20}$$

$$\beta_t \leqslant \dot{w}_t^d \quad \forall\, t \in T \tag{3.21}$$

$$\beta_t \cdot S \geqslant \dot{w}_t^d \quad \forall\, t \in T \tag{3.22}$$

Non-negativity Constraints:

$$0 \leqslant \theta_t,\ \beta_t,\ G_{t,\hat{t}} \leqslant 1 \quad \forall\, t, \hat{t} \in \hat{T} \tag{3.23}$$

$$\dot{w}_t,\ \dot{w}_t^c,\ \dot{w}_t^d,\ s_t,\ \kappa_{t,\hat{t}},\ y_{t,\hat{t}},\ \kappa_t^f \geqslant 0 \quad \forall\, t, \hat{t} \in \hat{T} \tag{3.24}$$

A number of cuts have been added to the model as seen in Eq.'s (3.18-3.22). These do not effect the working of the model but are incorporated to reduce the variable space of the problem, thereby reducing the computational time. Eq. (3.18)

states that there cannot be multiple half-cycles ending on the same time step. Eq.'s (3.19) and (3.21) ensure that the binary variables of charge (θ_t) or discharge (β_t)can take up the value 1 only when charging or discharging respectively, is actually occurring. Eq.'s (3.20) and (3.22) further link the charging and discharging binary variables to the power entering ($\dot{w}_t^c$) and leaving ($\dot{w}_t^d$) the battery respectively.

Finally, Eq. (3.23) & (3.24) are the non-negativity constraint that ensures none of the variables assume negative values.

Rolling time horizon and refinement of the model

The model uses a rolling time horizon so as to reduce the computational time and level of complexity. Further, the rolling time horizon allows us to refine the model by updating certain values for each period. In the model, an update period of 24 hours and a horizon of 36 hours are chosen. An update period of 24 hours is chosen due to the cyclic nature of PV systems, which are dependent on the sun and therefore, are repetitive each day. A horizon of 36 hours captures the next-day effects while limiting the large computational time that can be a result of longer horizons.The model calculates the capacity degradation of the battery. For each update period, the remaining capacity of the battery after degradation due to usage is calculated and stored as the new capacity of the battery. This new capacity value is updated in the model as the capacity of the battery for the next update period. In this manner, the optimization model uses more realistic battery capacity values, rather than using a single initial value for an entire year of data. The equation used

to calculate the capacity after degradation is:

$$S_{new} = S_{old} \cdot (1 - Degradation) \tag{3.25}$$

where S_{new} (kWh) is the new capacity of the battery after degradation, S_{old} (kWh) is the capacity of the battery before degradation, and *Degradation* is the fractional degradation of the battery in the latest update period.

The optimization model is formulated with an objective function in Eq. (3.3) that incorporates symmetry-breaking terms. However, these terms do not have any physical meaning, and an alternate objective is devised that better characterizes the desired outcome from the model. This objective function is stated in Eq. (3.26) and is calculated retrospectively for every update period. The profits made by power sent to the grid is calculated in a similar fashion as in the optimization model. The cost due to degradation of the battery is calculated by taking the initial battery capacity as an output from the model for every update period, calculating the new capacity due to degradation, and finding the difference. This is then multiplied by a cost factor, calculated based on the cost of eventually replacing the battery. Further, this cost of degradation is integrated into the objective function.

$$\sum_{t \in T} \{(\dot{w}_t + \gamma \cdot \dot{w}_t^d) \cdot K \cdot Z_t\} - \frac{(S_{old} - S_{new})}{S} \cdot \frac{CB}{1 - L} \tag{3.26}$$

where S (kWh) is the initial capacity of the battery, CB ($) is the cost of the battery, and L is the fractional EOL of the battery.

Eq.'s (3.25-3.26) are calculated in the post-processing after every update period

and are entered as parameters in the optimization model for the subsequent time period. Updating the new battery capacity due to degradation allows for a more realistic portrayal of the battery degradation as time progresses. Additionally, the post-processing objective (Eq. 3.26) more accurately calculates the net revenue. Therefore, both these equations help refines the model.

Linearizing non-linear nature of battery degradation

In addition to this, this work is being improved by introducing a multiplication factor to further increase the accuracy of the equation calculating degradation of the battery, by accounting for non-linear tendencies in the relation (Eq'.s (3.14a-3.15b)). This factor is to be derived by equating the slope of Eq'.s (3.14a-3.15b), multiplied by this factor (x), to the slope of a similar equation including a term related to the square of the number of cycles completed. On re-arranging this equation, the following is obtained:

$$x = \frac{A'_0 \cdot SOC_{start} + A'_1 \cdot SOC_{end} + A'_2 + A'_3 \cdot cycles}{A_0 \cdot SOC_{start} + A_1 \cdot SOC_{end} + A_2} \tag{3.27}$$

$A'_{0...3}$ and $A_{0...2}$ are constants. SOC_{start} and SOC_{end} are the starting and ending SOC, and *cycles* refers to the number of half-cycles completed. This multiplication factor accounts for long-term nonlinearity in the degradation graph by changing the slope of the equation over time. This allows the nonlinear nature of the graph of capacity versus the number of cycles of the battery for various start and end SOC to be accounted for in a linear manner within a given optimization horizon. The value of x will be updated in every update period since the slope changes with the

number of cycles of use.

Eq. (3.27) is calculated for every update period in the rolling time horizon and is fed into the model for the subsequent time period to more precisely portray the losses faced due to degradation. This method is yet to be applied in the model and has not been included in the current results. Further work will guarantee the viability of this approach.

Varied length of the two-dimensional set

With larger time horizons, it was realized that the two-dimensional set ($\hat{T}$) resulted in a large computational time. The presence of three two-dimensional variables ($G_{t,\hat{t}}, \kappa_{t\hat{t}}, y_{t\hat{t}}$) resulted in a large number of variables to run through all $t, \hat{t}$ combinations where $t, \hat{t} \in \hat{T}$. The two-dimensional variables were established to capture the time step in which the charge or discharge cycle begins (t) and ends ($\hat{t}$), in a single variable. This further facilitates the calculation of the degradation of the battery for every half-cycle, using the SOC at the start and end of the charge or discharge cycle. It was observed that more than one half-cycles took place in a single horizon and therefore, each half cycle typically lasted less than the length of the horizon (N_T). Therefore, to reduce the computational time, the optimization window of the two dimensional set was reduced. $\hat{T}$ was defined as the two-dimensional set of all time steps in the optimization window $\{t, t \ldots min(t + ts, N_T\}$. A number of ts values were experimented with, such that $t + ts < N_T$. In this method, the number of $t, \hat{t}$ combinations of the two-dimensional variables where significantly reduced. This in turn, reduced the computational time considerably. However, this resulted

in the model intentionally increasing the duration of many of the half-cycles so as to exclude them from the optimization window of the two-dimensional variables. Therefore, the start and end of the half-cycle could not be identified by a single variable and the model did not register the presence of these cycles. In turn, the model could not account for the degradation caused due to these unidentified cycles, resulting in an incorrect battery capacity and objective value. Further work is being done to constraint the half-cycles to take place within the optimization window. This has shown potential, yet requires additional efforts to perfect. Other alternatives, wherein longer half-cycles can be accounted for without sweeping through the entire horizon, are being explored as well.

"Rainflow" cycle counting method

The battery profile generated from the power generation system is irregular. When handling an irregular profile, a counting algorithm is necessary. The rainflow algorithm (Figure 3.2) is a commonly used method to count number of cycles over a time horizon, especially in structural engineering for fatigue analysis, mechanical vibration applications and power generation systems (Dragičević et al., 2014). The rainflow algorithm allows the irregular cycle to be divided into a number of regular cycles and categorizes each division based on the required property or feature (Sangwongwanich et al., 2017). For a battery profile, the rainflow algorithm allows the convenient categorizing of cycles based on starting SOC and ending SOC. The rainflow counting method uses the local maxima and minima to generate equivalent cycles. Therefore, it is conventionally used considering an entire time history of

load as the input, wherein the maximum and minimum values can be identified (Musallam and Johnson, 2012). This makes real-time applications of the rainflow algorithm difficult, since all the data must be presented to be able to locate the points of interest. The formulation of a real-time rainflow algorithm results in a recursive function, which further makes it difficult to implement in an optimization problem (Rosewater et al., 2019).

To understand the effect of this method and gauge its requirement, considering the challenges accompanying it, a nonlinear rainflow algorithm code is developed. This is further compared to a conventional cycle counting method. The start to end of charge or discharge is considered a half cycle as seen in the Figure 3.2. The battery capacity fade due to charge cycles for a number of sample battery profiles is calculated using each counting method and the difference in capacity fade is found.

Conventional cycle counting method

The conventional cycle counting method is an intuitive way to characterize cycling from a battery profile. The battery profile consists of charge half cycles and discharge half cycles. The starting point of each half cycle is chosen as the starting SOC and the ending point of each half cycle as the ending SOC, as seen in Figure 3.3. These are used in the equation to calculate the remaining capacity of the battery. Since the optimization occurs in real-time, the variable for number of cycles is accounted for as a half cycle. The starting and ending point of each half cycle can be seen in the Figure 3.3.

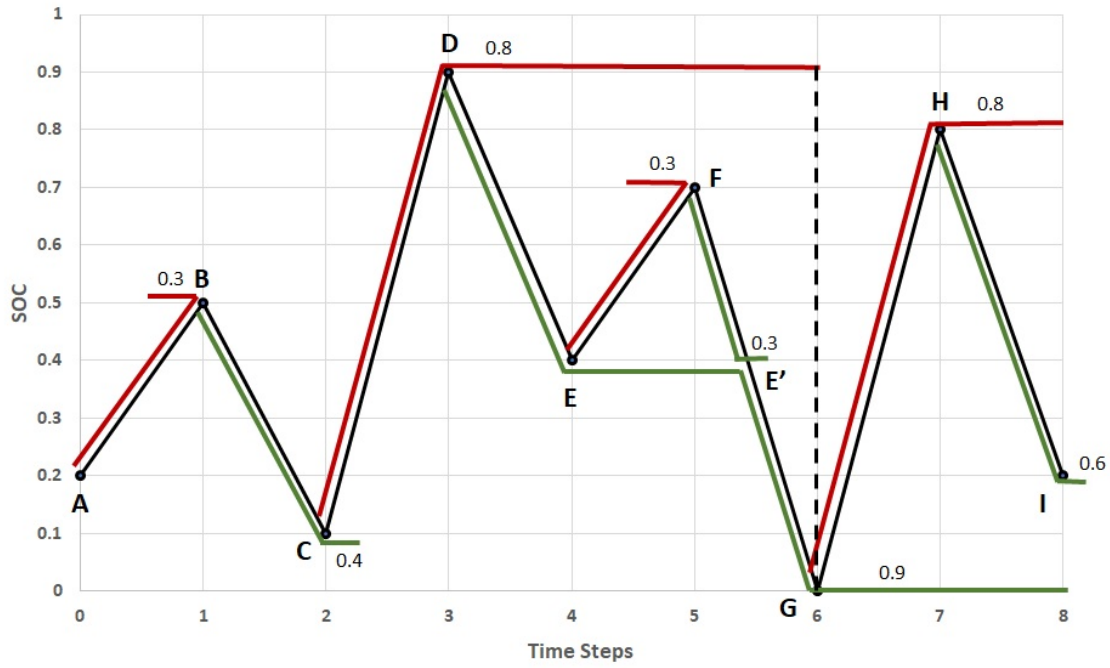

Points	SOC Range	Cycles
A-B	0.3	0.5
C-G	0.8	0.5
E-F + F-E	0.3	1
G-	0.8	0.5
B-C	0.4	0.5
D-G	0.9	0.5
H-	0.6	0.5

Figure 3.2: RAINFLOW CYCLE COUNTING METHOD. THE GRAPH SHOWS A BATTERY PROFILE AND HOW IT WOULD BE ANALYZED USING THE RAINFLOW ALGORITHM. THE TABLE FURTHER GROUPS THE DATA INTO FULL CYCLES AND REMAINING HALF CYCLES.

Algorithm 1: REGULAR CYCLE COUNTING METHOD

```
Input: Battery profile ;
def Regular(i, v, O_charge,max_charge val, p):
    for e in range of(0,len(O_charge) do
        SOC_charge = O_charge[e][1] - O_charge[e][0]
        change_in val charge.append([O_charge[e][0], O_charge[e][1], SOC_charge])
    end
```

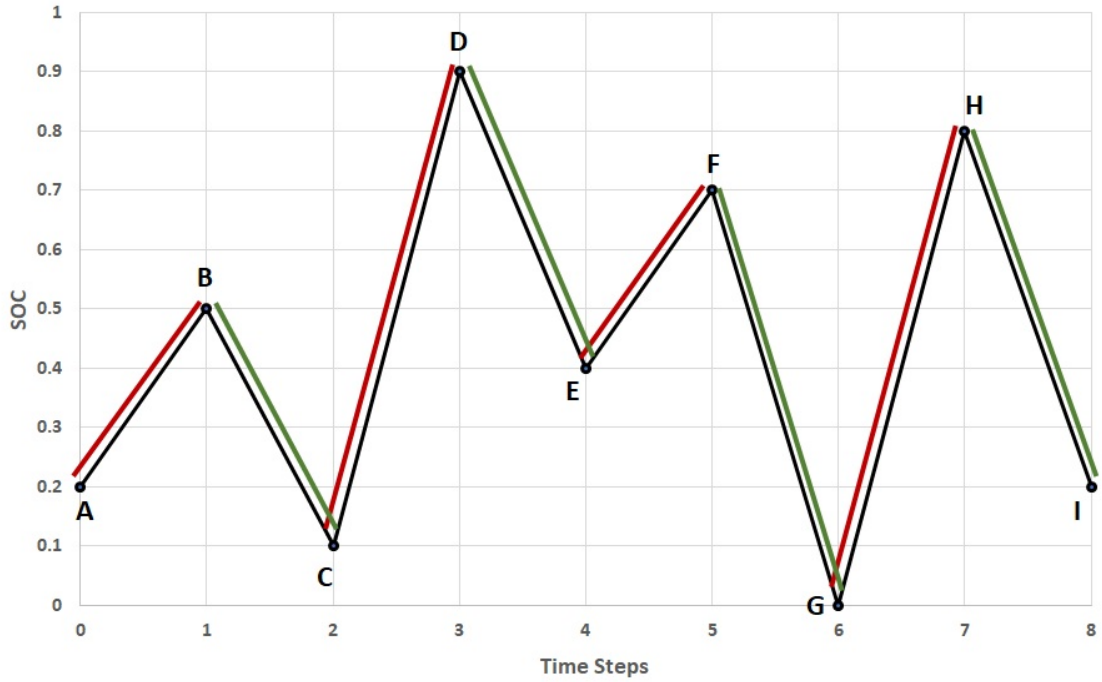

Points	SOC Range	Cycles
A-B	0.3	0.5
C-D	0.8	0.5
E-F	0.3	0.5
G-H	0.8	0.5
B-C	0.4	0.5
D-E	0.5	0.5
F-G	0.7	0.5
H-I	0.6	0.5

Figure 3.3: THE GRAPH SHOWS A BATTERY PROFILE AND DEMONSTRATES THE CONVENTIONAL CYCLE COUNTING METHOD TO ANALYZE THE START AND END POINTS OF EACH CHARGE OR DISCHARGE CYCLE.

Algorithm 2: RAINFLOW ALGORITHM

```
Input: Battery state of charge profile ;
def rainflow(i, v, O_charge, max_charge_val, p):
    while p < v and p > i do
        if O_charge[i][0] ⩾ O_charge[p][0]: then
            k ← i while k ⩾ i and k < p do
                if (O_charge[k][1] > max_charge_val) then
                    max_charge_val ← O_charge[k][1]
                    val ← k
                end
                k ← k + 1
                SOC_charge ← (max_charge_val - O_charge[i][0])
                APPEND(change_in_val_charge, [O_charge[i][0], max_charge_val, SOC_charge]
                )
                i ← i+1;       p←i+1;       m ← i;
                max_charge_val ← 0
                while m ⩾ i and m < (val+1): do
                    if O_charge[m][1] ⩾ O_charge[i-1][1]: then
                        maximum ← O_charge[i-1][1]
                        if (m-i)=0: then
                            SOC_charge ← (maximum - O_charge[i][0])
                            APPEND(change_in_val_charge,  [O_charge[i][0],  maximum,
                            SOC_charge] )
                            i ← i+1;       p ← i+1
                        else
                            minimum ← O_charge[i][0]
                            x ← i+1
                            while x > i and x < (m+1): do
                                if O_charge[x][0] < minimum: then
                                    minimum ← O_charge[x][0]
                                end
                                x ← x+1
                            end
                            if O_charge[i][0] = minimum: then
                                SOC_charge ← (maximum - O_charge[i][0])
                                APPEND(change_in_val_charge,  [O_charge[i][0],  maximum,
                                SOC_charge] )
                                i ← i+1;       p ← i+1;
                                t,w,q ← rainflow(i, m+1, O_charge, 0, p) ; // Recursive entry
                                point
                                i ← w;       p ← q;
                                SOC_charge ← (O_charge[i-1][1] - O_charge[i][0])
                                APPEND(change_in_val_charge,  [O_charge[i][0],  maximum,
                                SOC_charge] )
                                i ← i+1;       p ← i+1;
                            else
                                t,w,q ← rainflow(i, m+1, O_charge, 0, p) ; // Recursive entry
                                point
                                i ← w;       p ← q;
                                SOC_charge ← (maximum - O_charge[i][0])
                                APPEND(change_in_val_charge,  [O_charge[i][0],  maximum,
                                SOC_charge] )
                                i ← i + 1;       p ← i+1;
                            end
                        end
                    end
                    m ← m+1
                end
            end
        else
            p ← p+1
        end
    end
    return [change_in_val_charge, i, p]
```

Rolling time horizon optimization model

The rolling time horizon is an approach used to reduce the computation time on mathematical models having long time horizons (Marquant et al., 2015). This approach solves the problem in a periodic manner. In this method, the problem is split into a number of smaller time periods or horizons. However, the horizon must be selected appropriately, based on repetitive patterns in the data, so as to ensure the validity of the results. The method of the rolling time horizon can be understood from Figure 3.4. In the Figure, H denotes the length of a horizon, which is the number of time steps over which the model would be solved. From the data produced by the model, for the time horizon H, the information for the time period U (the update period) is stored. Therefore, the decisions made for time period U, are taking in consideration the scheduling and occurrences of the larger time period H. The time horizon is then rolled by the update period U and this process is repeated for the total number of time steps.

Through the rolling time horizon approach, the computational load of the model is significantly reduced into smaller sections. In addition to this, by having a larger horizon than the update period, we ensure that optimization decisions can incorporate future events and reduce the "end effects" of solving the model piecewise, compared to computing the model for the update period alone. However, the use of a rolling time horizon can compromise the accuracy of the results to a certain extent (GLOMB et al., 2010). To reduce this inaccuracy, the horizon should be selected with care. For a PV optimization model, the regularity in the energy produced makes it easier to select a time horizon that reduces the level of

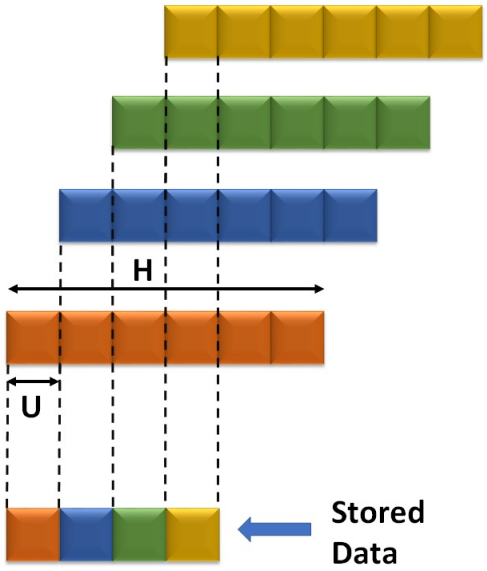

Figure 3.4: ROLLING TIME HORIZON OPTIMIZATION DESCRIPTION

inaccuracy. Therefore, by adopting this method, the computation time of the model is significantly reduced, improving the applicability and accessability of the model.

4 RESULTS

In this thesis, two main factors are tested: (a) the comparison between the rainflow algorithm and the conventional cycle counting algorithm, and (b) the results of the dispatch optimization model developed in this work. The approach used for cycle counting in the optimization model depends on the results of the comparison of the two counting algorithms. Hence, this is discussed prior to the final results of the optimization model.

Comparison and verification of conventional cycle counting method

A battery charge and discharge profile generated from SAM's PVWatts-Battery Residential model is used as an input (Figure 4.1) and the number of charge cycles and other associated variables are counted using the rainflow algorithm and the conventional cycle counting method. This was done for one year worth of data, using hourly time steps. The capacity of the battery after degradation due to charge cycles is calculated for time periods ranging from one week to 52 weeks at one week intervals, using both the rainflow algorithm and the conventional cycle counting method. The results are plotted in Figure 4.2. Further, the difference in final capacity of the battery after degradation due to charge cycles for various durations of usage is also tabulated (Figure 4.2).

When comparing the two cycle counting methods, the total number of cycles counted by each method should ideally be the same, and this was proven to be true.

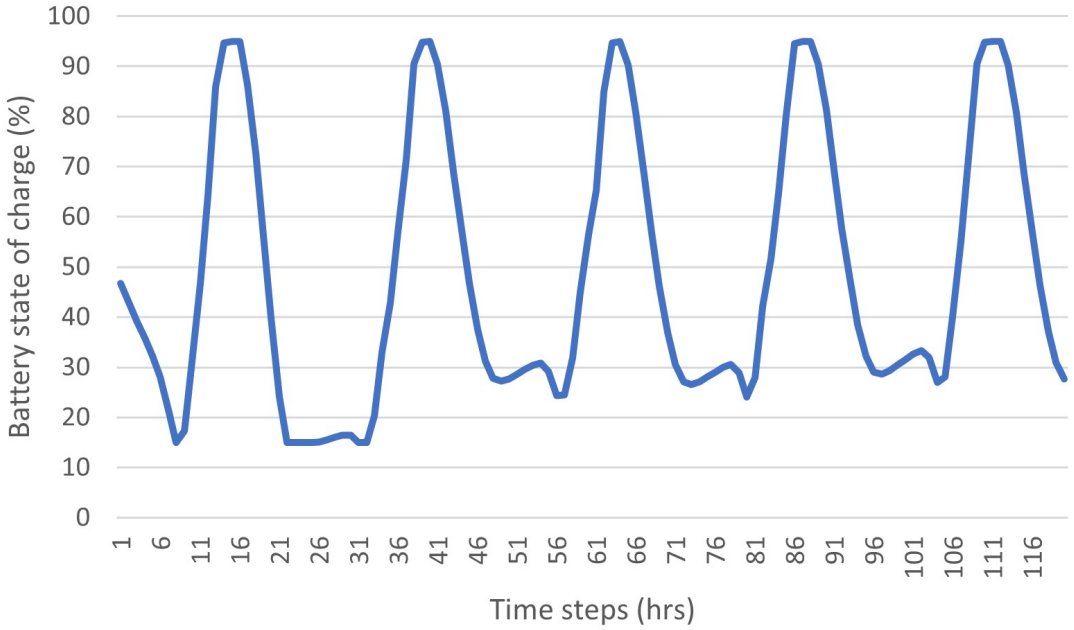

Figure 4.1: BATTERY PROFILE GENERATED BY SAM'S PV WATTS-BATTERY RESIDENTIAL MODEL SHOWING THE SOC % OF THE BATTERY FOR EVERY HOUR FOR A PERIOD OF FIVE DAYS.

The difference essentially lies in the points identified as the starting and ending SOC for each cycle. This influences the capacity of the battery after degradation due to the fact that start and end SOC are terms in the equation used to calculate the final capacity of the battery (Eq.'s (3.14a-3.15b)). On observing Figure 4.2, however, it can be seen that the difference in final capacity of the battery for various durations, considering charge cycles, is very small. The average difference in SOC identified by the two methods is 1.6% – an amount that has a nearly insignificant effect on the capacity degradation of the battery. Over a duration of a year, the difference in capacity degradation of the battery due to charge cycles using the two

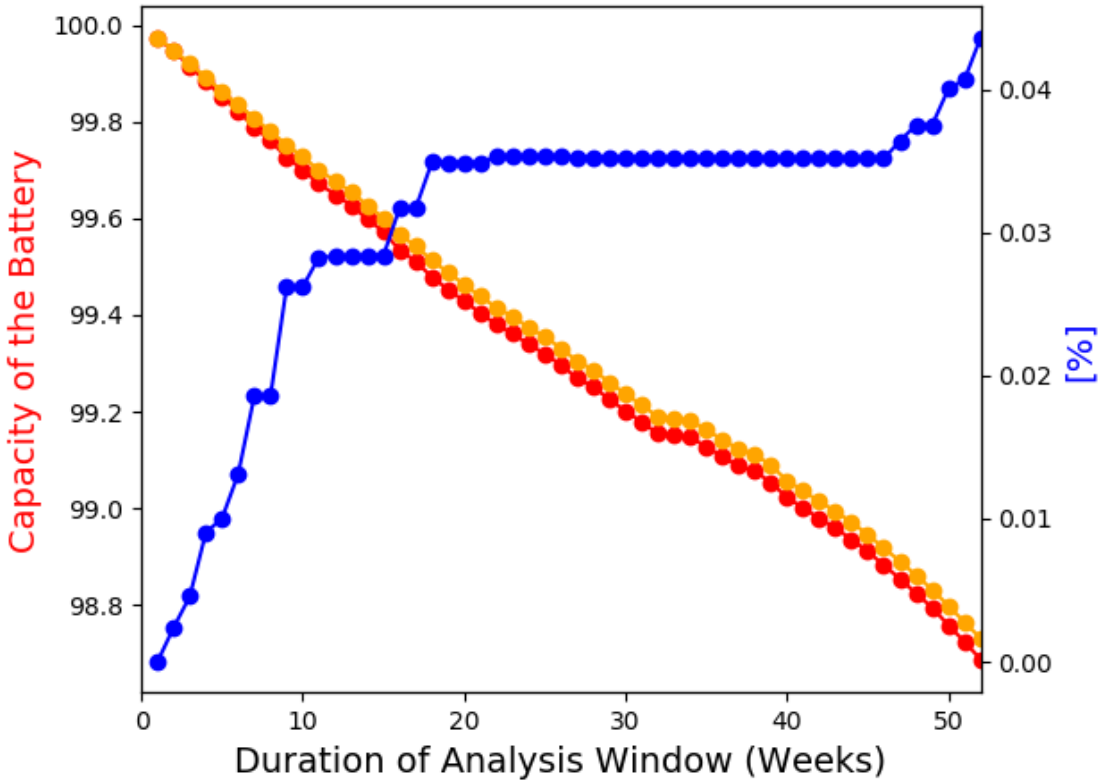

Figure 4.2: CAPACITY PERCENT OF THE BATTERY FOR VARYING DURATION OF ANALYSIS USING RAINFLOW ALGORITHM AND CONVENTIONAL COUNTING METHOD AND THE DIFFERENCE OF THE TWO.

cycle counting methods is seen to be 0.044%. Therefore, it is observed that the use of the conventional cycle counting method for this battery type and application does not sacrifice accuracy while reducing the computational and coding complexity significantly. This is mostly due to the fact that the rainflow algorithm is especially beneficial in studies where cycles are grouped based on a certain parameter or variables. In many battery degradation studies, the battery degradation is calculated based on certain other variables (such as energy throughput), which requires

careful categorizing. In this work, however, the battery degradation is calculated on a per-cycle basis. Therefore, the difference between the rainflow algorithm and the conventional cycle counting method is not significantly felt. Hence, for the model developed in this thesis, the conventional cycle counting method is selected to analyze the battery profile.

Base-case optimal scheduling results

The dispatch optimization model developed in this thesis is tested using model data produced by SAM as the input power generated by the hypothetical PV system. The model is run for a time horizon of 36 hours as well as 24 hours (for comparison purposes) and an update period of 24 hours over the course of one year. Upon completion, the model provides the final capacity of the battery after degradation and the objective function (that maximizes the profits) as results.

Specific solver setting were used in Gurboi to reduce the computational time of the model. These were as follows:

Table 4.1: SOLVER SETTINGS

Solver Settings	**Set Values**
Parallel threads	4
Cuts	3
MIPGap	0.01
Time limit	360 seconds

The number of parallel thread to apply depends on the number of cores in the machine. Additionally, since two jobs were run simultaneously, 4 threads were chosen for this job. Aggressive cuts were used and set to the maximum, that is

3 for very aggressive cut generation. Further, the MIPGap was set to 0.01 so that the solver will terminate when the gap between the lower and upper bound is less than the MIPGap multiplied by the absolute value of the incumbent objective value. Finally, the time limit, restricts the total time that can be spent on a run. When one horizon solves for 360 seconds, it is terminated with the best solution available as the output. With the above described settings, the model was able to solve to optimality for a 24 hour horizon, although it usually achieved the set MIPGap in under 60 seconds for each horizon. However, a 36 hour horizon reached the maximum solver time limit before reaching optimality. Therefore, the solutions presented for a 36 hour horizon could be improved by allowing a longer solver time for the model to solve to optimality. However, the increased run time is more tedious and reduces usability. Future work is targeted to improve the model and solver settings so that the optimal solution can be obtained within shorter run time.

A secondary dispatch model, without battery lifetime optimization, is compared to the model developed in this work. The secondary model does not consider battery lifetime implications in the objective function when utilizing the battery and only attempts to maximize the profits obtained through the dispatch of electricity to the grid. This is done to realize the differences in the battery use and dispatch trends of the battery without battery lifetime optimization, when compared to the usage of the battery from the model with battery lifetime optimization. Both the final battery capacity due to degradation and the net revenue are compared. The model consists of an objective function similar to Eq. 3.3, sans the variables involved in tracking the cycles of the battery and the degradation of the battery.

Maximize:

$$\sum_{t \in T} \left(\dot{w}_t + \gamma \cdot \dot{w}_t^d \right) \cdot Z_t \cdot K \tag{4.1}$$

The constraints are represented by Eq.'s (3.4-3.7). The same input data is then fed into this secondary dispatch optimization model. The results from the secondary dispatch model without battery lifetime optimization is then post-processed to calculate the degradation of the battery. This degradation is multiplied by a cost factor (the same used in the primary dispatch optimization model that considers battery lifetime optimization, developed in this work) and subtracted from the objective function. In this manner, the final capacity of the battery after degradation and the maximized profits (including the cost associated with battery degradation) are generated as results. The results from the two dispatch models (with and without battery lifetime optimization) are compared.

Upon comparing the two models, it is seen in Figure 4.3 that the dispatch model with battery lifetime optimization improves battery life significantly. In the following calculations, it is assumed that 80% capacity is the EOL of the battery. The dispatch model with battery lifetime optimization results in a degradation of 0.77% of the battery capacity while the dispatch model without battery lifetime optimization results in a degradation of 3.30%. This shows that the battery degradation has been reduced by 77.73% by including battery lifetime optimization in the dispatch model. If a similar trend is maintained every year (due to similarities in the solar behavior each year), it can be extrapolated that the battery used without battery lifetime optimization will reach the EOL in 6 years. On the other hand, the battery used in the dispatch model with lifetime optimization will reach its EOL in 27 years.

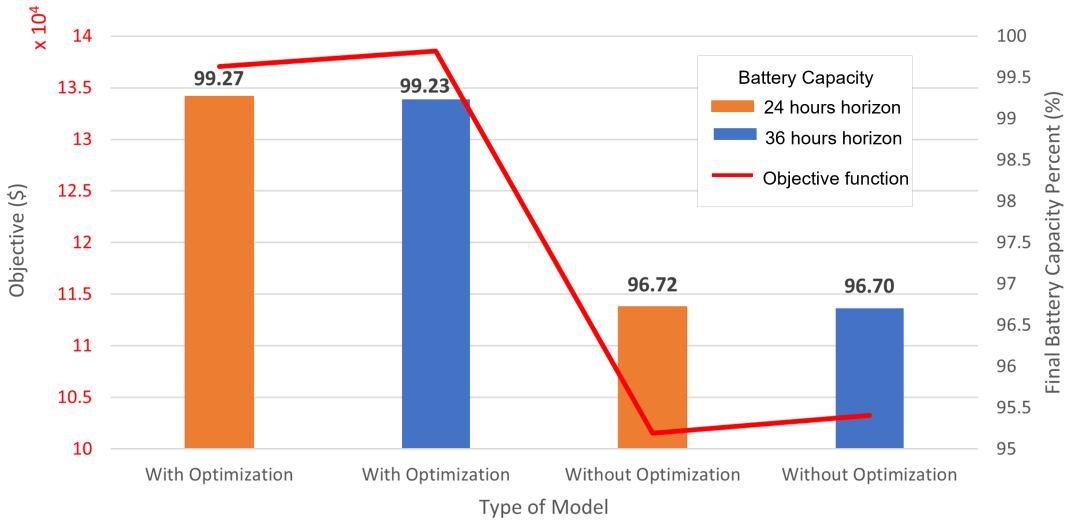

Figure 4.3: FINAL BATTERY CAPACITY PERCENT AND OBJECTIVE OBTAINED BY THE DISPATCH MODEL WITH AND WITHOUT BATTERY LIFETIME OPTIMIZATION FOR ONE YEAR OF DATA WITH A 24 HOUR HORIZON AND A 36 HOUR HORIZON

This shows a significant improvement in the life of the battery used in the dispatch model with battery lifetime optimization and clearly portrays the importance of having such a model. This is further emphasized on comparing the net revenue resulting from both the models. The net revenue is obtained by adding the profits obtained from the dispatch of power to the grid, to the losses due to the cost of eventually replacing the battery when it reaches EOL. The dispatch model with battery lifetime optimization results in an increase in revenue by 34.17%.

From the Figure 4.4 it can be seen that the battery in the model without lifetime optimization has been used much more aggressively than the model with lifetime optimization. This allows for an increased profit by allowing the model to store the

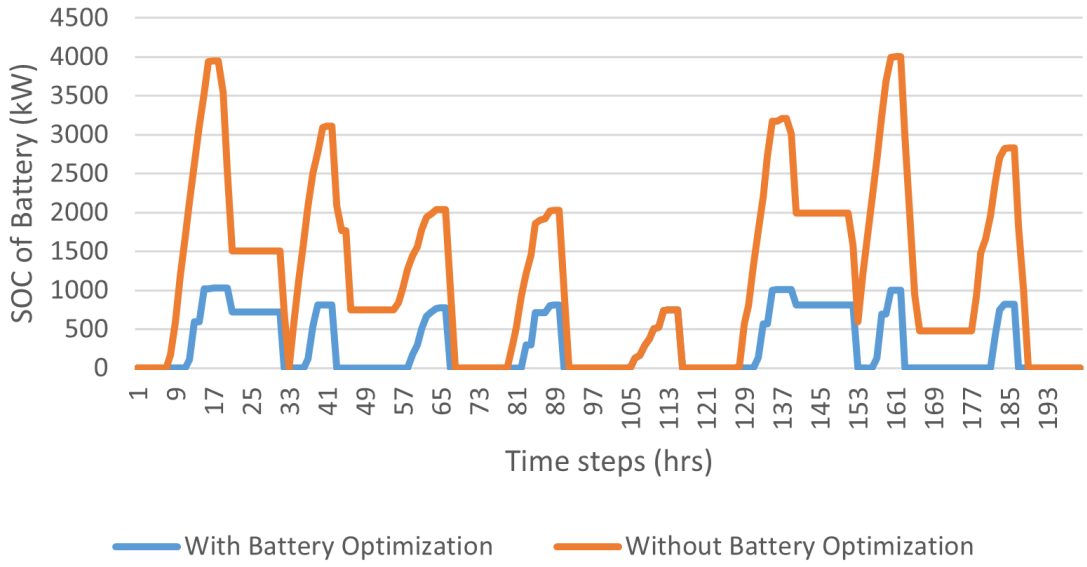

Figure 4.4: COMPARISON OF THE BATTERY PROFILE GENERATED FROM THE DISPATCH MODEL WITH BATTERY LIFETIME OPTIMIZATION AND WITHOUT BATTERY LIFETIME OPTIMIZATION.

power produced at times with a lower revenue multiplier (Z_t) and dispatch the power from the battery at time steps with a higher revenue multiplier (Z_t). While this increases the profits obtained through the dispatch of power, it also increase the losses associated with the replacement of the battery, by increasing the battery degradation through the extreme use of the battery. On the other hand, when the dispatch model with battery lifetime optimization is exposed to a revenue multiplier (Z_t), with certain time steps exhibiting negative pricing, the model chooses to do "nothing," resulting in the wastage of power from the PV array as seen in time steps 7 to 8 in Figure 4.5. This implies that the cost associated with the degradation of the battery due to charging in that time step does not justify the profits (through

later dispatch), and the model would rather waste the power in that time step.

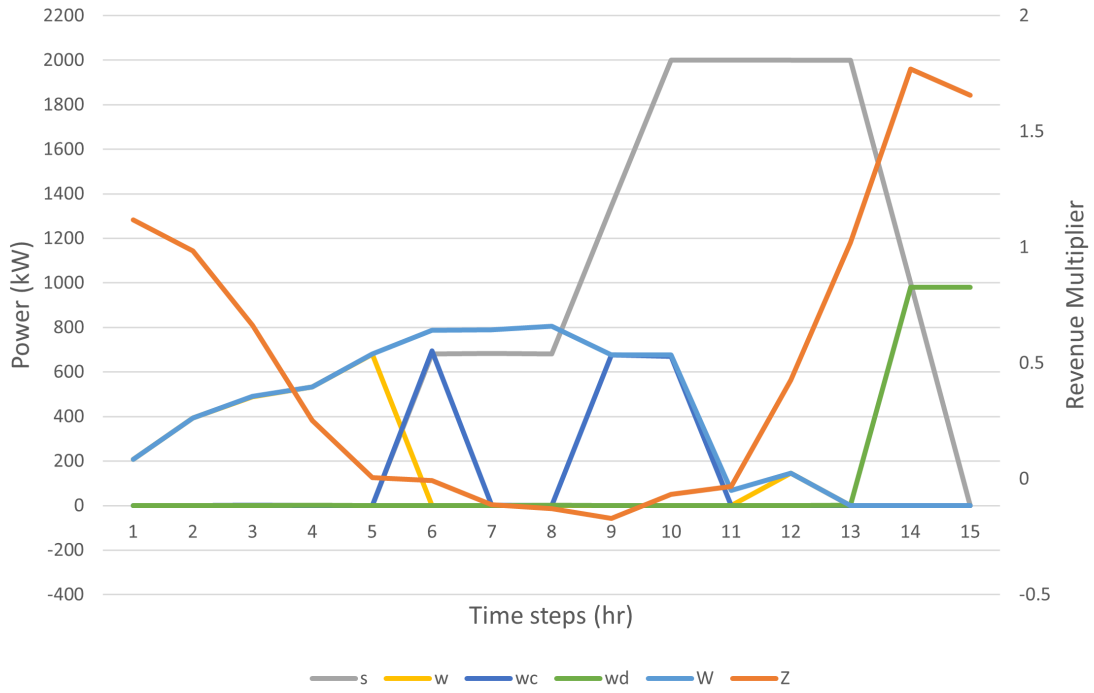

Figure 4.5: POWER FLOW FROM THE PV SYSTEM, TO AND FROM THE BATTERY, POWER FLOW TO THE GRID AND THE REVENUE MULTIPLIER VALUES FOR DIFFERENT TIME STEPS

Further, on comparing the 24 hour horizon with the 36 hour horizon, Figure 4.3 shows that the difference in final battery capacity percent is noticeable in both types of models, along with a small increase in the total revenue (1.11% increase). The small difference in final values could be due to similar patterns of the sun each day. Allowing the solver to run for a longer solve time for a 36 hour horizon to reach optimality, may produce a more pronounced difference in results (when compared to 24 hour horizon). Hence, the beneficial impact of day-ahead scheduling, although

seen in this comparison, may be better realized by using longer horizons. Further research would reveal if longer horizons will continue to improve the results or if the benefits of the longer horizon begin to neutralize beyond a certain point.

Sensitivity Studies

Three sensitivity studies were conducted by varying the input parameters in the dispatch model with battery lifetime optimization. The three parameters studied were the grid limit (kW), the cost of the battery per kWh ($/kWh) and the initial battery capacity (kWh). Each parameter was run for a number of values for a period of one year with a 24 hour horizon as well as a 36 hour horizon. Graphs were made comparing the parameter values with the final battery capacity and the final objective function (net revenue).

Three values of the grid limit were compared: 500 (kW), 750 (kW) and 1000 (kW). A higher grid limit allows for more power to be sent to the grid in each time step, which results in an increased objective function value (Figure 4.7). For the battery profiles generated using the different grid limits, the lower grid limit (500 (kW)) constrains the amount of power that can be discharged by the battery in single time step. This can severely impact the objective by limiting the power discharge in time steps with higher revenue multipliers, thereby reducing the profits to be made. This explains the lower objective obtained by the dispatch model with 500 (kW) as the grid limit.

Higher grid limits allow a larger discharge of power in the time steps with a larger revenue multiplier resulting in greater profits. However, the difference in

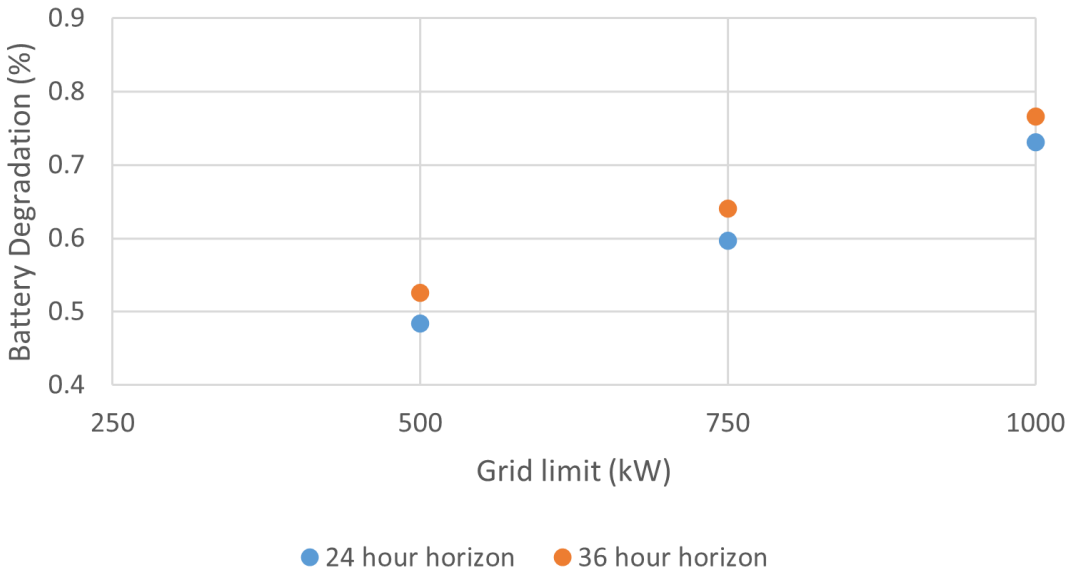

Figure 4.6: SENSITIVITY STUDY COMPARING THE GRID LIMIT TO THE FINAL BATTERY DEGRADATION PERCENT OBTAINED FROM THE MODEL.

profits between 750 (kW) and 1000 (kW) is less significant due to the limitation placed by the net power generated by the PV system. Although the higher grid limit allows more power to be discharged from the battery to the grid – which would result in a greater profit – the power in the battery depends on the power generated by the PV system. The hourly results of the model show that the power generated by the PV system in a 36 hour horizon does not often (but does sometimes) charge the battery to a 1000 (kW). Therefore, the difference in objective function between the 750 (kW) and 1000 (kW) grid limit is small, as the limitations imposed by the PV system dominate those of the grid limit.

A similar explanation can be extended to the relationship between the usage of

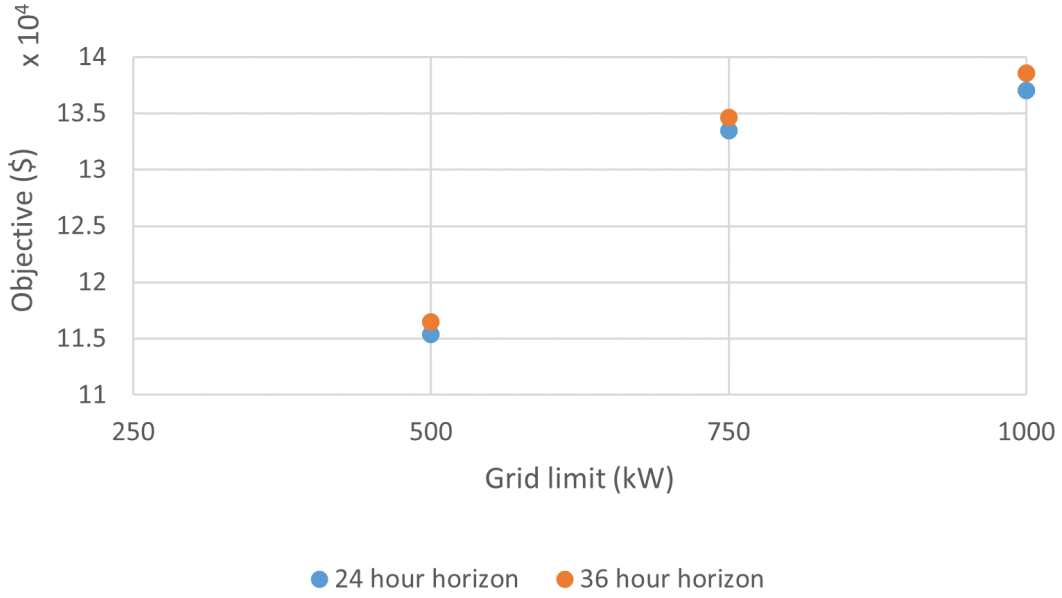

Figure 4.7: SENSITIVITY STUDY COMPARING THE GRID LIMIT TO THE FINAL OBJECTIVE OBTAINED FROM THE MODEL.

the battery and the grid limit. The model choses to store power in the battery to discharge it at time steps with a higher revenue multiplier. However, the lower grid limit reduces the amount of power that can be dispatched in these select time steps. Hence, the model does not have the incentive to charge the battery to a higher SOC as the battery can only discharge up to the grid limit.This results in a lower battery utilization for lower grid limits, as can be seen in Figure 4.6.

This was followed by comparing three values of the cost of the battery: 150 ($/kWh), 225 ($/kWh) and 300 ($/kWh). Figure 4.8 revealed that a lower cost battery resulted in the highest degradation of the battery. This behavior is expected, as a lower-cost battery will result in a lower penalty for degradation (and eventual

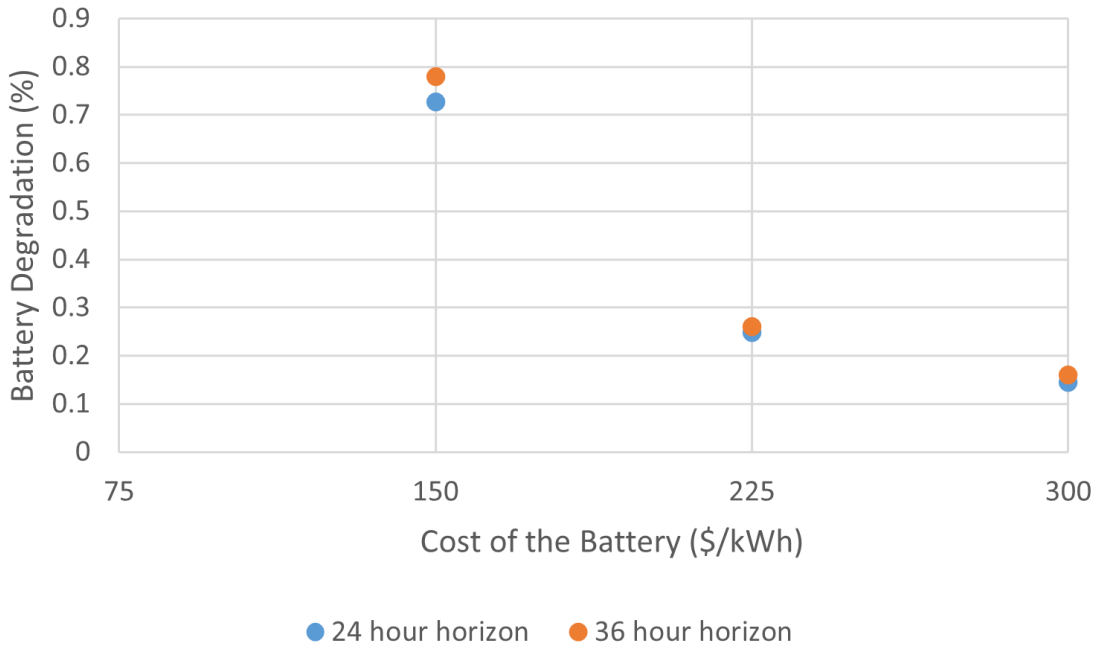

Figure 4.8: SENSITIVITY STUDY COMPARING THE COST OF THE BATTERY TO THE FINAL BATTERY DEGRADATION PERCENT OBTAINED FROM THE MODEL.

battery replacement) in the objective function. The low cost of the battery allows for more liberal utilization. The higher battery usage results in an increased profit from dispatch of energy, and despite higher degradation, the objective function is higher, as shown in Figure 4.9. This is because the cost of the battery is lower and the cost of the high degradation is outweighed by the benefit of producing additional energy during more profitable hours.

As the battery cost increases (to 225 $/kWh and 300 $/kWh), the difference between the results reduce. The benefits of the low cost of the battery are relative to the cost of electricity. As the cost of the battery increases, it becomes increasingly

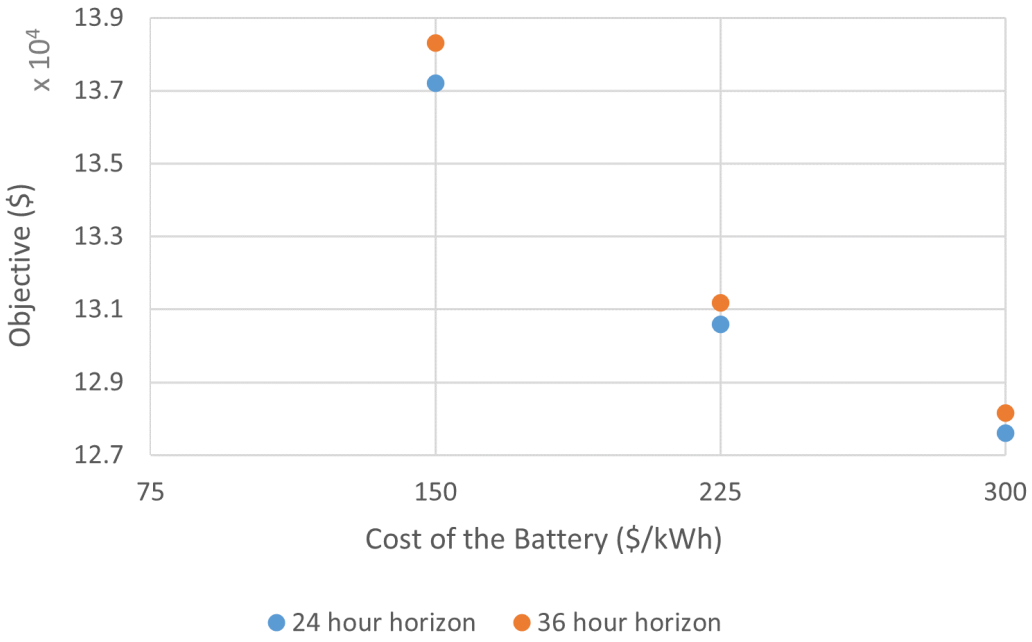

Figure 4.9: SENSITIVITY STUDY COMPARING THE COST OF THE BATTERY TO THE FINAL OBJECTIVE OBTAINED FROM THE MODEL.

difficult for the profits of dispatch of power from the battery, to outweigh the loss due to degradation. Beyond a certain battery cost it is expected that the battery profiles will become nearly uniform. A similar result is reflected in the final objective. The difference in the final objective reduces as the battery cost increases. Therefore, the relation between the cost of the battery and both the results, is a non-linear one.

In the final case study, two values of initial battery capacity were chosen: 1000 (kWh) and 4000 (kWh). Figure 4.10 shows that the dispatch model with a lower initial battery capacity results in a significantly higher degradation than the model beginning with a higher battery capacity. This is because a battery with a smaller initial capacity will have to be used more extensively with a greater number

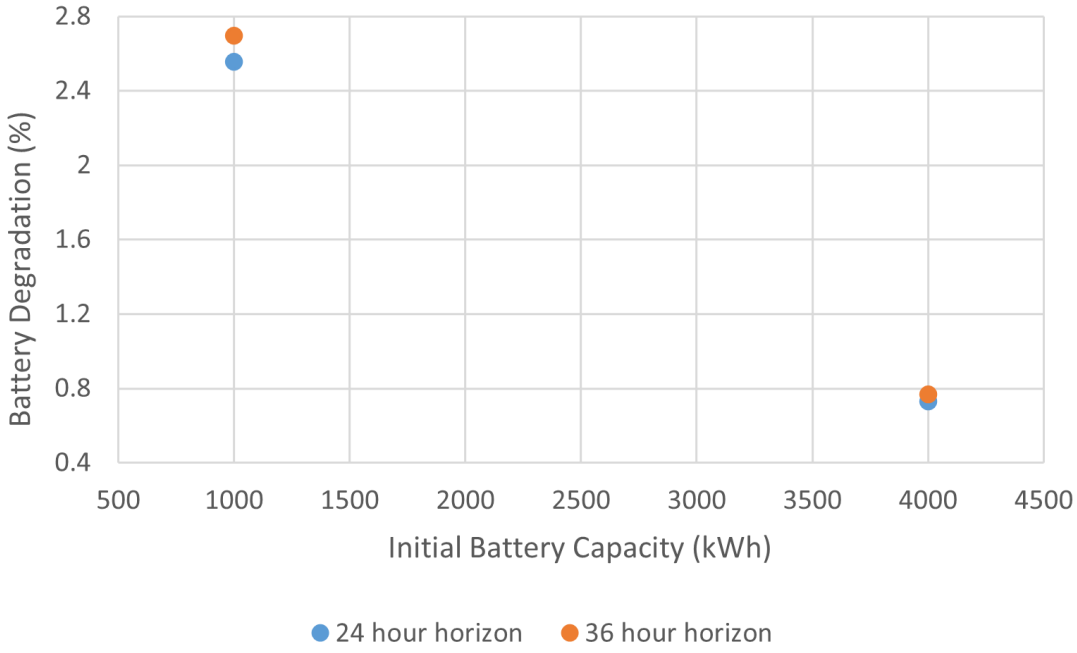

Figure 4.10: SENSITIVITY STUDY COMPARING THE INITIAL BATTERY CAPACITY TO THE FINAL BATTERY DEGRADATION PERCENT OBTAINED FROM THE MODEL.

of charge and discharge cycles to achieve a significant dispatch of power to the grid when compared to a battery with a higher initial capacity. In addition to this, a battery with a lower initial capacity will cost less since the cost is on a per kWh capacity basis. Therefore, the penalty of degradation is reduced, allowing the model to use the battery more aggressively and profit from it.

The effect of this is seen in Figure 4.11. The final objective obtained by the model using the 1000 (kWh) initial battery capacity is greater than that obtained using the 4000 (kWh) initial battery capacity. Therefore, the lower cost of the battery with a lower initial battery capacity significantly impacts the final objective of the model

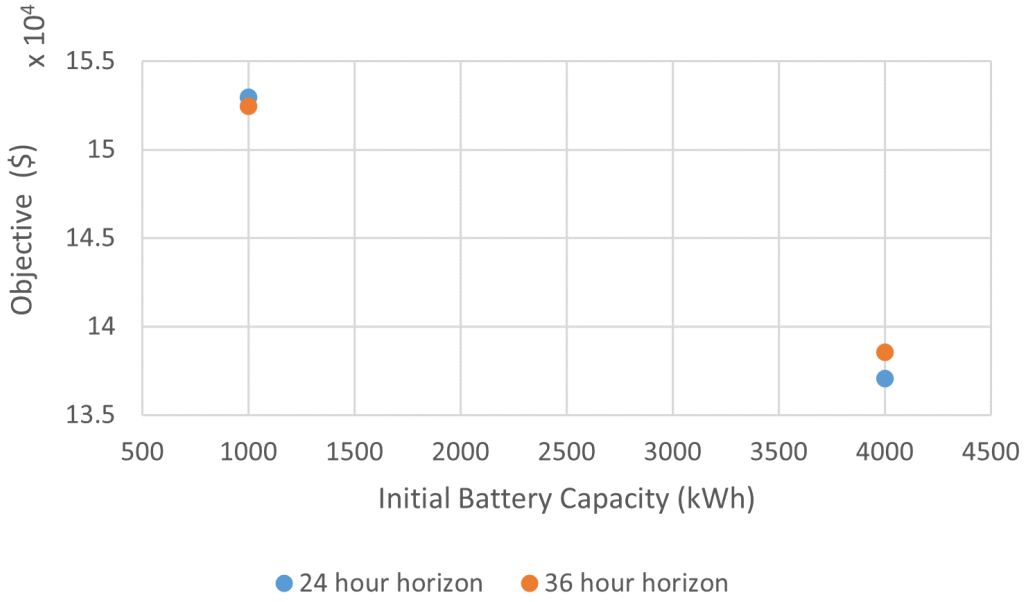

Figure 4.11: SENSITIVITY STUDY COMPARING THE INITIAL BATTERY CAPACITY TO THE FINAL OBJECTIVE OBTAINED FROM THE MODEL.

and proves to be beneficial to obtain higher profits. This, once again, highlights the importance of a battery degradation model in a dispatch optimization model.

Altogether, the sensitivity studies reveal that varying certain parameters changes the behavior of the battery and results in a different net revenue. The results obtained further validate the functioning of the dispatch model. Specific values of the parameters have resulted in more favorable outcomes than others. With regards to the cost of the battery, it is confirmed by the model that a lower cost of the battery improves the net revenue of the model, although it corresponds to an increased rate of degradation of the battery. With respect to the grid limit, a higher grid limit results in a greater net revenue while also causing a greater degradation

of the battery. When the initial battery capacity is observed, a lower initial battery capacity results in a increased battery degradation and net revenue. Further, in most of the comparisons of the 24 hour horizon with the 36 hour horizon, the 36 hour horizon degrades the battery more than the 24 hour horizon, but results in a larger net revenue. This would be because the longer horizon allows for the model to plan and discharge the battery, carrying on beyond the 24 hour period, at time steps with higher revenue multipliers, thereby increasing the profits but also using the battery more extensively. This result is seen for all the studies, save the case where the initial battery capacity is 1000 (kWh). In this case, the 24 hour horizon leads to less degradation but an increased net revenue when compared to a 36 hour horizon. This could be because the low battery capacity limits the requirement and capability (due to limited power stored) to carry over power to the following horizon, reducing the effectiveness of the 36 hour horizon. It would be interesting to study longer horizons to observe if the same trend continues.

Since the net revenue accounts for the cost of eventually replacing the battery, it is proven that in the cases with a higher objective and increased degradation, the increased use of the battery was justified, resulting in higher profits. Therefore, the cases with increased revenue are more favorable despite the increased degradation of the battery.

5 CONCLUSION

This thesis develops a hybrid renewable generator optimization model with integrated battery lifetime optimization. This is accomplished using a mixed-integer-linear program written in Pyomo and solved using Gurobi. The objective of the model is to maximize the profits made by the dispatch of electricity to the grid, while also accounting for the loss due to the cost of eventually replacing the battery. Various variables affecting the cyclic aging of the battery are studied and it is shown that high and low SOC, as well increased number of cycles caused degradation of the battery. Therefore, an equation characterizing the capacity degradation of the battery in terms of these variables (SOC and number of cycles) is developed and used in the battery lifetime optimization model. By doing so, the model ensures a more cost-effective use of the battery, thereby extending the expected lifetime of the battery.

This thesis also compares the rainflow algorithm to a conventional cycle counting method to determine whether the simpler conventional algorithm is appropriate for analyzing the battery profile in the model. We observe that the two cycle-counting methods predict a difference of 0.044% in battery degradation over a time period of one year. This value being negligible, we conclude that the conventional cycle counting method can be adopted in the decision optimization model, thereby eliminating the computational difficulties involved with implementing the rainflow algorithm in a mixed-integer-linear program.

The dispatch model with battery lifetime optimization was analyzed by com-

paring it to a similar model without battery lifetime optimization. The final battery capacity after degradation due to usage and the final objective function, including the profits made by the dispatch of power to the grid and the loss due to the cost of eventually replacing the battery, were compared. The base case comparison of one year of data revealed that model with battery lifetime optimization reduced the battery degradation by 77.73%. If it is assumed that the similar results are produced each year, the EOL of the battery can be predicted. The battery used in the model without battery lifetime optimization will reach EOL in 6 years, while the battery in the model with battery lifetime optimization will last 27 years. Further, one year of data showed that the model with battery lifetime optimization improved the net revenue (objective function) by 34.17%. This shows that the cost of the battery largely impacts the cost of the system and a model without battery lifetime optimization leads to unrealized losses. Therefore, a dispatch model, with battery lifetime optimization results in an increased and more accurate net revenue than a dispatch model without battery lifetime optimization.

A sensitivity study was carried out to test understand how various parameters effected the models objective function and the final battery capacity. In most cases, an increased objective was obtained by the more aggressive use of the battery. The eventual dispatch of power from the battery resulted in an increased objective function as well as more degradation of the battery. It was seen that a higher grid limit resulted in a better objective. In addition to this, a lower battery cost was seen to give a greater objective. Similarly, a battery with a lower initial battery capacity (which inturn would reduce the cost of the battery) resulted in an increased

objective and battery degradation. Finally, it was seen in most of the sensitivity studies as well as the base case, that a 36 hour horizon resulted in an improved objective when compared to a 24 hour horizon, proving that day-ahead scheduling does improve the model. Yet, longer horizons must be tested to find the optimum horizon for day-ahead scheduling in this hybrid dispatch models using PV systems.

With the increased usage of renewable energy systems that are accompanied by energy storage, the necessity of battery lifetime optimization models has been greatly amplified. The results in this thesis establish the effectiveness and the importance of such models in improving the life of the battery and ensuring its efficient use, in addition to maximizing net profit.

6 FUTURE WORK

The research conducted in this thesis leaves a large scope for future studies. There are a number of areas that can be improved upon to increase the efficiency and robustness of the model. Two of the key areas based on the results are the detail associated with the characterizing of the degradation of the battery, and the computational time of the model. The characterization of the degradation of the battery can be made more detailed by accounting for cyclic aging as well as calendar aging (while this work only accounts for cyclic aging). In addition to this, further research must be conducted to better understand the parameters and variables that effect the aging of the battery and how these parameters and variables corelate with the final capacity of the battery mathematically. This would result in a more accurate portrayal of the reduced battery capacity due to degradation.

As mentioned in the methodology, future work will attempt to more precisely portray the non-linear relationship between the number of cycles and the degradation of the battery for various starting and ending SOC. To accomplish this, a correction factor can be introduced and updated in every update period of the model to capture the slope of the degradation relation that changes with the number of cycles of use. The total number of battery cycles is compounded at the end of the update period, and this cumulative cycle count is used to calculate the correction factor in the post processing after every update period. This factor is then fed into the model in the subsequent update period, thereby changing the slope of the degradation constraint. This technique is still being tested to incorporate in the

model.

The large computational time requirement of the program hinders usability to some extent, and the requirement of a commercial solver, such as Gurobi, reduces its accessability. The increased computational time is mainly due to the presence of two-dimensional (especially binary) variables that result in an exponential increase in the optimization model complexity. The two-dimensional variables are present to identify all $t,\ \hat{t}$ combinations in which t is the starting SOC of the charge or discharge cycle and $\hat{t}$ is the ending SOC of the charge or discharge cycle. Attempts to narrow this window based on trends in battery usage has been discussed in the methodology chapter. The two-dimensional variables occupy the largest computational time and attempts are being made to reduce the extensiveness of the two-dimensional set, thereby reducing the problem complexity. One promising approach involves redefining the $\hat{T}$ set to include only the time steps in smaller optimization window, as shown in Eq. 6.1.

$$\hat{T} = \{t, t \dots \min(t + ts, N_T)\} : t + ts < N_T \tag{6.1}$$

This allows the two-dimensional variables to be calculated for fewer $t,\ \hat{t}$ combinations. The challenge being faced by this method is that the model intentionally extends the charge or discharge half-cycles to last longer than the optimization window so that the battery behavior and degradation is not be captured by the two-dimensional variables assigned to this task. Further work is required to overcome this challenge, but the proposed method to reduce the computational time shows promise and further work can determine the viability.

The two-dimensional variables that are responsible for the large computational time are present to characterize the degradation in the battery. In addition to this, many of the mathematical equations relating battery capacity to working parameters and variables are non-linear in nature. Making these non-linear equations linear is often challenging and can sometimes lead to increased solver times due to the additional constraints that are introduced for linearization. Therefore, it can be extrapolated based on this, as well as literature((Goebel et al., 2016)) that increased detail in the model and the nature of the equations characterizing the degradation of the battery, often results in an increased computational time. The battery degradation in this model was chosen to balance the two aspects, attempting to deliver higher accuracy with regards to the battery degradation without an exorbitant computational time. Further research could reduce the solve time by developing more efficient ways to represent the degradation of the battery while also incorporating additional expressions to present a more detailed characterization of battery degradation with use.

REFERENCES

Barré, Anthony, Benjamin Deguilhem, Sébastien Grolleau, Mathias Gérard, Frédéric Suard, and Delphine Riu. 2013. A review on lithium-ion battery ageing mechanisms and estimations for automotive applications. *Journal of Power Sources* 241:680–689.

Belt, J, V Utgikar, and I Bloom. 2011. Calendar and phev cycle life aging of high-energy, lithium-ion cells containing blended spinel and layered-oxide cathodes. *Journal of Power Sources* 196(23):10213–10221.

Bordin, Chiara, Harold Oghenetejiri Anuta, Andrew Crossland, Isabel Lascurain Gutierrez, Chris J Dent, and Daniele Vigo. 2017. A linear programming approach for battery degradation analysis and optimization in offgrid power systems with solar energy integration. *Renewable Energy* 101:417–430.

bp Statistical Review of World Energy. 2021. bp statistical review of world energy. `https://www.bp.com/en/global/corporate/energy-economics/statistical-review-of-world-energy.html`.

Buller, Stephan, Marc Thele, Eckhard Karden, and Rik W De Doncker. 2003. Impedance-based non-linear dynamic battery modeling for automotive applications. *Journal of Power Sources* 113(2):422–430.

Denholm, Paul, R Margolis, and J Milford. 2008. Production cost modeling for high levels of photovoltaics penetration. Tech. Rep., National Renewable Energy Lab.(NREL), Golden, CO (United States).

Denholm, Paul, Matthew O'Connell, Gregory Brinkman, and Jennie Jorgenson. 2015. Overgeneration from solar energy in california. a field guide to the duck chart. Tech. Rep., National Renewable Energy Lab.(NREL), Golden, CO (United States).

DiOrio, Nicholas A, Janine M Freeman, and Nate Blair. 2018. Dc-connected solar plus storage modeling and analysis for behind-the-meter systems in the system advisor model. In *2018 ieee 7th world conference on photovoltaic energy conversion (wcpec)(a joint conference of 45th ieee pvsc, 28th pvsec & 34th eu pvsec)*, 3777–3782. IEEE.

Dragičević, Tomislav, Hrvoje Pandžić, Davor Škrlec, Igor Kuzle, Josep M Guerrero, and Daniel S Kirschen. 2014. Capacity optimization of renewable energy sources and battery storage in an autonomous telecommunication facility. *IEEE Transactions on Sustainable Energy* 5(4):1367–1378.

Ecker, Madeleine, Nerea Nieto, Stefan Käbitz, Johannes Schmalstieg, Holger Blanke, Alexander Warnecke, and Dirk Uwe Sauer. 2014. Calendar and cycle life study of li (nimnco) o2-based 18650 lithium-ion batteries. *Journal of Power Sources* 248:839–851.

Fathima, A Hina, and K Palanisamy. 2015. Optimization in microgrids with hybrid energy systems–a review. *Renewable and Sustainable Energy Reviews* 45:431–446.

Ferroukhi, Rabia, Alvaro Lopez-Peña, Ghislaine Kieffer, Divyam Nagpal, Diala Hawila, Arslan Khalid, Laura El-Katiri, Salvatore Vinci, and An-

dres Fernandez. 2016. Renewable energy benefits: Measuring the economics. https://www.irena.org/-/media/Files/IRENA/Agency/Publication/2016/IRENA_Measuring-the-Economics_2016.pdf.

Fortenbacher, Philipp, Johanna L Mathieu, and Göran Andersson. 2014. Modeling, identification, and optimal control of batteries for power system applications. In *2014 power systems computation conference*, 1–7. IEEE.

Freeman, Janine M., Nicholas A. DiOrio, Nathan J. Blair, Ty W. Neises, Michael J. Wagner, Paul Gilman, and Steven Janzou. 2018. System Advisor Model (SAM) General Description (Version 2017.9.5). Tech. Rep., National Renewable Energy Lab.(NREL), Golden, CO (United States).

Ghorbanzadeh, Milad, Majid Astaneh, and Farzin Golzar. 2019. Long-term degradation based analysis for lithium-ion batteries in off-grid wind-battery renewable energy systems. *Energy* 166:1194–1206.

GLOMB, LUKAS, FRAUKE LIERS, and FLORIAN ROSEL CA. 2010. A rolling-horizon approach for multi-period optimization. *Mine*.

Goebel, Christoph, Holger Hesse, Michael Schimpe, Andreas Jossen, and Hans-Arno Jacobsen. 2016. Model-based dispatch strategies for lithium-ion battery energy storage applied to pay-as-bid markets for secondary reserve. *IEEE Transactions on Power Systems* 32(4):2724–2734.

Goodall, Gavin, Michael Scioletti, Alex Zolan, Bharatkumar Suthar, Alexandra Newman, and Paul Kohl. 2019. Optimal design and dispatch of a hybrid microgrid system capturing battery fade. *Optimization and Engineering* 20(1):179–213.

Goodenough, John B, and Youngsik Kim. 2010. Challenges for rechargeable li batteries. *Chemistry of materials* 22(3):587–603.

Guena, T, and P Leblanc. 2006. How depth of discharge affects the cycle life of lithium-metal-polymer batteries. In *Intelec 06-twenty-eighth international telecommunications energy conference*, 1–8. IEEE.

Kassem, Mohammad, Julien Bernard, Renaud Revel, Serge Pelissier, François Duclaud, and C Delacourt. 2012. Calendar aging of a graphite/lifepo4 cell. *Journal of Power Sources* 208:296–305.

Laresgoiti, Izaro, Stefan Käbitz, Madeleine Ecker, and Dirk Uwe Sauer. 2015. Modeling mechanical degradation in lithium ion batteries during cycling: Solid electrolyte interphase fracture. *Journal of Power Sources* 300:112–122.

Lasseter, Robert H. 2007. Microgrids and distributed generation. *Journal of Energy Engineering* 133(3):144–149.

Lu, Languang, Xuebing Han, Jianqiu Li, Jianfeng Hua, and Minggao Ouyang. 2013. A review on the key issues for lithium-ion battery management in electric vehicles. *Journal of power sources* 226:272–288.

Maheshwari, Arpit, Nikolaos G Paterakis, Massimo Santarelli, and Madeleine Gibescu. 2020. Optimizing the operation of energy storage using a non-linear lithium-ion battery degradation model. *Applied Energy* 261:114360.

Marquant, Julien F, Ralph Evins, and Jan Carmeliet. 2015. Reducing computation time with a rolling horizon approach applied to a milp formulation of multiple urban energy hub system. *Procedia Computer Science* 51:2137–2146.

Merei, Ghada, Cornelius Berger, and Dirk Uwe Sauer. 2013. Optimization of an off-grid hybrid pv–wind–diesel system with different battery technologies using genetic algorithm. *Solar Energy* 97:460–473.

Millner, Alan. 2010. Modeling lithium ion battery degradation in electric vehicles. In *2010 ieee conference on innovative technologies for an efficient and reliable electricity supply*, 349–356. IEEE.

Musallam, Mahera, and C Mark Johnson. 2012. An efficient implementation of the rainflow counting algorithm for life consumption estimation. *IEEE Transactions on reliability* 61(4):978–986.

Ouyang, Minggao, Xuning Feng, Xuebing Han, Languang Lu, Zhe Li, and Xiangming He. 2016. A dynamic capacity degradation model and its applications considering varying load for a large format li-ion battery. *Applied Energy* 165:48–59.

Palacín, M Rosa, and Anne de Guibert. 2016. Why do batteries fail? *Science* 351(6273).

Ploehn, Harry J, Premanand Ramadass, and Ralph E White. 2004. Solvent diffusion model for aging of lithium-ion battery cells. *Journal of The Electrochemical Society* 151(3):A456.

Rosewater, David, Alexander Headley, Frank Austin Mier, and Surya Santoso. 2019. Optimal control of a battery energy storage system with a charge-temperature-health model. In *2019 ieee power & energy society general meeting (pesgm)*, 1–5. IEEE.

Sangwongwanich, Ariya, Yongheng Yang, Dezso Sera, and Frede Blaabjerg. 2017. Lifetime evaluation of grid-connected pv inverters considering panel degradation rates and installation sites. *IEEE transactions on Power Electronics* 33(2):1225–1236.

Schoenung, Susan. 2011. Energy storage systems cost update. *SAND2011-2730* 606.

Sengupta, Manajit, Yu Xie, Anthony Lopez, Aron Habte, Galen Maclaurin, and James Shelby. 2018. The National Solar Radiation Data Base (NSRDB). *Renewable and Sustainable Energy Reviews* 89:51–60.

Sharma, Namit, Bram Smeets, and Christer Tryggestad. 2019. The decoupling of gdp and energy growth: A ceo guide. *McKinsey Quarterly* 1–11.

Smith, Kandler, E Wood, S Santhanagopalan, GH Kim, J Neubauer, and A Pesaran. 2014. Models for battery reliability and lifetime. Tech. Rep., National Renewable Energy Lab.(NREL), Golden, CO (United States).

Swierczynski, Maciej, Daniel-Ioan Stroe, Ana-Irina Stan, Remus Teodorescu, and Søren Knudsen Kær. 2015. Lifetime estimation of the nanophosphate $LiFePO_4/C$ battery chemistry used in fully electric vehicles. *IEEE Transactions on industry Applications* 51(4):3453–3461.

U.S. Census Bureau, Imports of Petroleum. 2021. U.S. Census Bureau, Imports of Petroleum. `https://www.census.gov/foreign-trade/statistics/historical/petro.pdf`. Accessed: 2021-06-10.

Wang, John, Ping Liu, Jocelyn Hicks-Garner, Elena Sherman, Souren Soukiazian, Mark Verbrugge, Harshad Tataria, James Musser, and Peter Finamore. 2011. Cycle-life model for graphite-lifepo4 cells. *Journal of power sources* 196(8):3942–3948.

Wikner, Evelina, and Torbjörn Thiringer. 2018. Extending battery lifetime by avoiding high soc. *Applied Sciences* 8(10):1825.

Xu, Bolun, Alexandre Oudalov, Andreas Ulbig, Göran Andersson, and Daniel S Kirschen. 2016. Modeling of lithium-ion battery degradation for cell life assessment. *IEEE Transactions on Smart Grid* 9(2):1131–1140.

Zhao, Bo, Xuesong Zhang, Jian Chen, Caisheng Wang, and Li Guo. 2013. Operation optimization of standalone microgrids considering lifetime characteristics of battery energy storage system. *IEEE transactions on sustainable energy* 4(4):934–943.

Zheng, Yong, Yan-Bing He, Kun Qian, Baohua Li, Xindong Wang, Jianling Li, Cui Miao, and Feiyu Kang. 2015. Effects of state of charge on the degradation

of lifepo4/graphite batteries during accelerated storage test. *Journal of Alloys and Compounds* 639:406–414.